AN APPROACH TO BIS(AMINO ACID)S UTILIZING DIMETHYL

2,4-BIS(DIAZO)-3-OXOGLUTARATE AND STUDIES OF

TRIS(2,6-DIHYDROXYPHENYL)E, E = B, P.

Except where reference is made to the work of others, the work described in this thesis is my own or was done in collaboration with my advisory committee. This thesis does not include proprietary or classified information.

_____
Lirui Guan

Certificate of Approval:

_____   _____
Edward J. Parish   Peter D. Livant, Chair
Professor   Associate Professor
Chemistry   Chemistry

_____   _____
Thomas E. Albrecht-Schmitt   Stephen L. McFarland
Associate Professor   Dean
Chemistry   Graduate School

AN APPROACH TO BIS(AMINO ACID)S UTILIZING DIMETHYL

2,4-BIS(DIAZO)-3-OXOGLUTARATE AND STUDIES OF

TRIS(2,6-DIHYDROXYPHENYL)E, E = B, P.

Lirui Guan

A Thesis

Submitted to

the Graduate Faculty of

Auburn University

in Partial Fulfillment of the

Requirements for the

Degree of

Master of Science

Auburn, Alabama

December 16, 2005

AN APPROACH TO BIS(AMINO ACID)S UTILIZING DIMETHYL

2,4-BIS(DIAZO)-3-OXOGLUTARATE AND STUDIES OF

TRIS(2,6-DIHYDROXYPHENYL)E, E = B, P.

Lirui Guan

_____

Signature of Author

_____

Date

iii

THESIS ABSTRACT

AN APPROACH TO BIS(AMINO ACID)S UTILIZING DIMETHYL

2,4-BIS(DIAZO)-3-OXOGLUTARATE AND STUDIES OF

TRIS(2,6-DIHYDROXYPHENYL)E, E = B, P.

Lirui Guan

Master of Science, December 16, 2005
(B.S., Hunan Univeristy, 2001)

84 typed pages

Directed by Peter D. Livant

When treated with a diazo transfer agent, dimethyl 3-oxoglutarate afforded a high yield of the bis(diazo) compound dimethyl 2,4-bis(diazo)-3-oxoglutarate, 33. The bis(diazo) compound, catalyzed by $Rh_2(OAc)_4$, reacted with an excess of O-benzyl carbamate, ($CbzNH_2$), to give the product of double N-H insertion, 36, [MeO_2C-CH(NHCbz)]$_2$C=O. Thus in two steps one obtains a protected bis(amino acid). Compound 36 exhibits complex ^{1}H and ^{13}C NMR spectra, which may be rationalized by assuming 36 is predominantly enolic.

Attempted removal of the Cbz protecting groups gave startling results. Hydrogenation of 36 over Pd/C led to dimethyl 2-carboxamidosuccinate, 44,

MeO$_2$CCH$_2$CH(CONH$_2$)(CO$_2$Me), the structure of which was proven by x-ray crystallography.

In other studies, tris(2,6-dimethoxyphenyl)boron was synthesized by literature procedures. Demethylation was attempted using AlCl$_3$/toluene, and BBr$_3$·SMe$_2$. In both cases, resorcinol, the product of B-C bond cleavage was observed.

Tris(2,6-dihydroxyphenyl)phosphonium chloride 63 was synthesized and its x-ray crystal structure was determined. It binds ethyl ether via a hydrogen bond. The three aryl rings adopt propeller symmetry, with torsion angles relative to the P-H direction of 20.5°, 24.5°, and 30.8°. Compared to the average C-P-H angle of [Ph$_3$PH]$^+$ - 108.2°, the average C-P-H angle of 63 is smaller, namely 104.9°.

ACKNOWLEDGMENT

I would like to thank Dr. Peter Livant who has been so helpful in my research here at Auburn University, Dr. Albrecht-Schmitt for assistance with X-ray crystallography and Dr. Parish for his help with the thesis. I also would like to give the thanks to my laboratory partners Mrs. Yuanping Jie, Mr. Hui Wang and Mr. Xiaoxun Li for their help in my research. Also thank to my wife for supporting my life.

Style manual or journal used: Journal of Organic Chemistry

Computer software used: Microsoft Word 2002 & Chem. Draw Ultra 7.0

TABLE OF CONTENTS

LIST OF SCHEMES

LIST OF FIGURES

LIST OF TABLES

1. PART I. INTRODUCTION

1.1 Introduction to Diazocarbonyl Compounds

The date of the first recorded synthesis of an α-diazocarbonyl compound is from the work of Curtius[1,2] on diazotization of natural α-amino acids (ethyl diazoacetate was first synthesized in 1883 from glycine). The simple diazocarbonyl compounds became available only in the late 1920s with the work of Arndt and Eistert,[3-5] and of Bradley and Robinson.[6] Now, modern organic synthesis continues to benefit from the unique versatility of diazocarbonyl compounds in cyclopropanation, X-H insertion (X = C, N, O, S, Se, P, halogen), Wolff rearrangement, ylide formation with subsequent transformations, aromatic cycloaddition and substitution, and many other useful reactions.

There are perhaps four principal reasons for the high level of activity in the diazo compound area. First, the enormous number of transformations that can occur with diazocarbonyl compounds makes them extremely versatile reactants. Second, methodology for their synthesis has continued to develop on a broad front, and there are now available well-tested, reliable procedures for the preparation of all the main classes of diazocarbonyl compounds. Third, the introduction in the 1970s of dirhodium(II) catalysts for diazocarbonyl decomposition opened up numerous new opportunities for highly chemoselective transformations that were largely inaccessible with

conventionalcopper catalysts. Fourth, the ever-increasing demands for stereocontrol in the production of molecules of high enantiopurity have led to the introduction of chiral catalysts for asymmetric transformations of diazocarbonyl compounds.[7]

The synthesis of diazoketones involves addition of an acyl chloride to ethereal diazomethane[3-5] at or below 0 °C (eq. 1). Numerous synthetic intermediates containing the diazoketone functional group have been obtained in this way.

$$RCOCl \ + \ 2\,CH_2N_2 \quad \xrightarrow[0\,°C]{Et_2O} \quad RCOCHN_2 \ + \ CH_3Cl \ + \ N_2 \qquad (1)$$
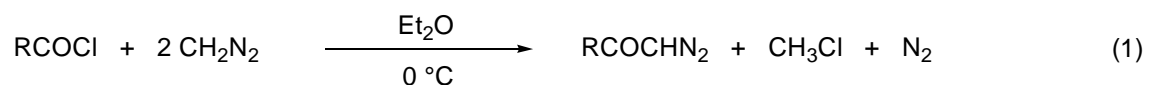
1.2 Diazo Transfer Reaction

Diazo transfer is now the standard route which is widely used to transfer a complete diazo group from a donor to an acceptor. Since the middle of the last century, sulfonyl azide compounds have been developed to serve as excellent diazo donors.[8] The diazo group transfers to the α-methylene position of a carbonyl compound by the simple diazo transfer procedure of direct exposure to tosyl azide in dry acetonitrile or ethanol using triethylamine as a base (eq. 2).

$$(2)$$
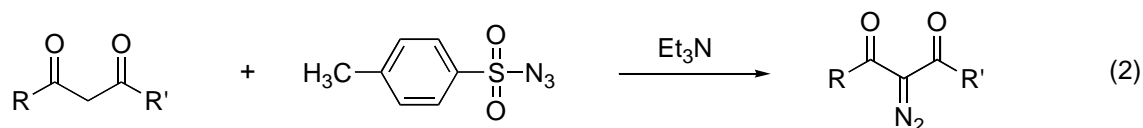
The mechanism of diazo transfer reaction has been developed by M. Regitz

Saarbrücken (Scheme 1).[9]
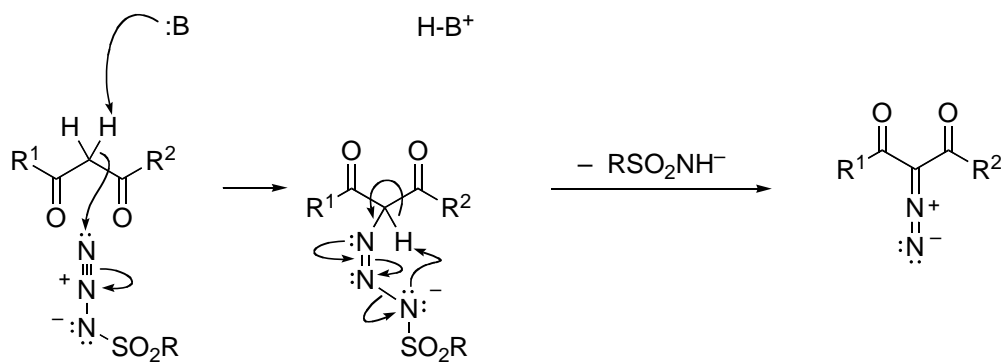
Scheme 1

Although tosyl azide has been by far the most frequently employed diazo donor,

and was used by Doering and DePuy in 1953 in their synthesis of

diazocyclopentadiene,[10] work in the Merck laboratories[11] has raised doubts regarding the

safety aspects of this reagent. With these worries, Merck chemists[11,12] have examined

sulfonyl azides **1** to **12** from the standpoint of utility, thermal stability, ease of handling,

and safety. It was found that methanesulfonyl (mesyl) azide **1** was the most hazardous

and dangerous diazo transfer reagent of the group. Compared to more dangerous transfer

reagent, tosyl azide, *p*-acetamidobenzenesulfonyl azide (*p*-ABSA) **7** offers more safety,

yield, and ease of manipulation in diazo transfer. This reagent is currently commercially

available and has some advantage in safety and yield, and so it is used in our laboratory

for the diazo transfer reactions. These diazo transfer reagents, **1** to **12**, are very efficient,

giving good yield (>80%) in various diazo transfer reactions.

CH₃SO₂N₃

$CH_3SO_2N_3$

1

2

3

4

5

6

7

8

9

10

11

12
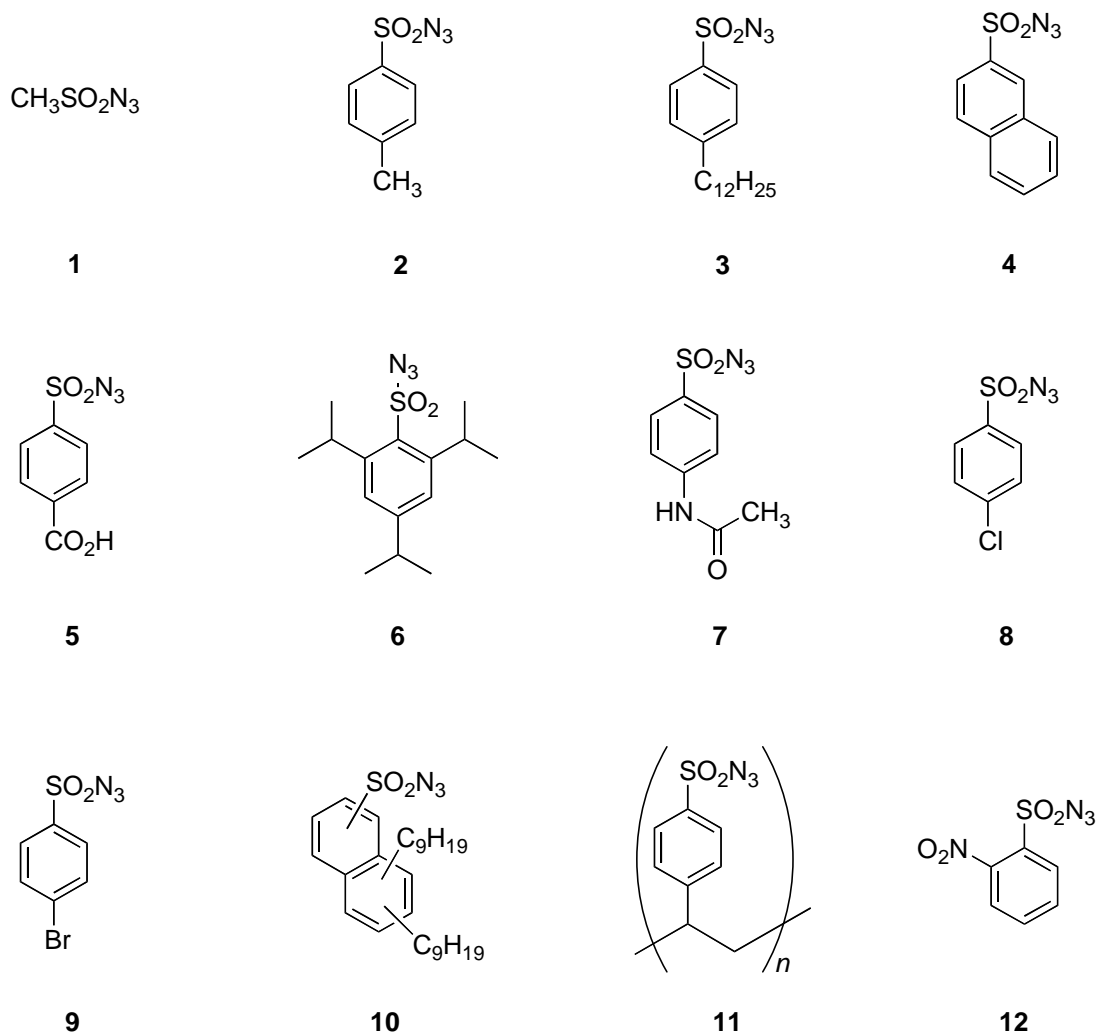
These diazo transfer reagents may be made from the corresponding sulfonyl chlorides (eq. 3).
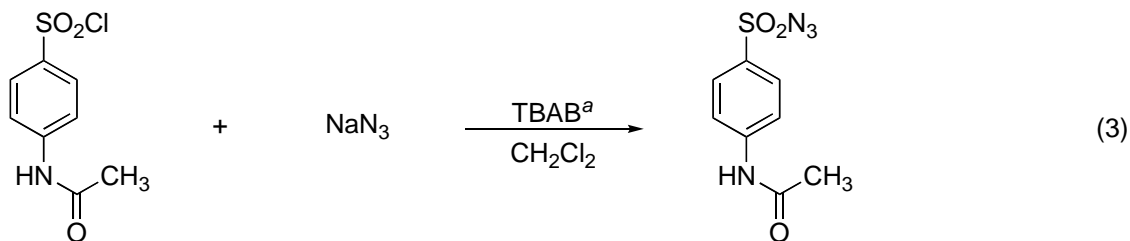
^{a} tetrabutylammonium bromide

(3)

7

With a diazo transfer reagent such as **7**, the α-diazocarbonyl compound is readily formed. When the reaction site is activated by *two* flanking carbonyls, the diazo transfer reaction works even more successfully. For example, Hazen et al.[11] employed the naphthalene-based diazo transfer reagent **4** in the high-yield synthesis of dimethyl diazomalonate, DDM (eq. 4).

DDM, 95%

(4)
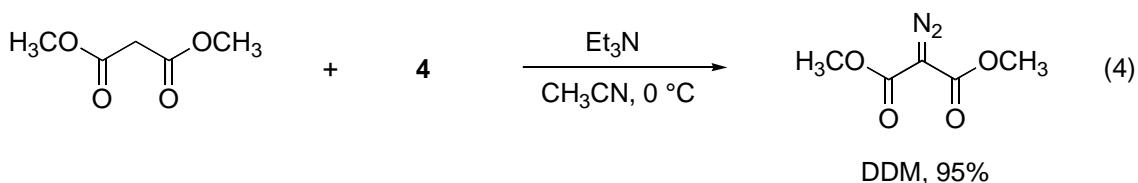
1.3 Catalysts for Metal Carbene Transformations

Diazo compounds are inherently unstable to acid-promoted decomposition. Transition metals, which act as Lewis acids, are therefore effective catalysts for diazo decomposition.[14] The reactivities of diazocarbonyl compounds and alkyl/aryl diazo compounds are different. This may be rationalized on the basis of the pK_a values of the corresponding diazonium ions. As an example, diazomethane is the conjugate base of the methanediazonium ion (eq. 5), whose pK_a value[14] of 10 suggests the driving force for the

high reactivity of diazomethane towards Brønsted acids, and, by extension, Lewis acids.

$$\underset{\underset{H}{|}}{\overset{\overset{H}{|}}{H-C-\overset{+}{N}\equiv N}} \quad \rightleftharpoons \quad \underset{\underset{H}{|}}{\overset{\overset{H}{\diagdown}}{C=\overset{+}{N}=\overset{-}{N}}} \quad + \quad H^+ \tag{5}$$
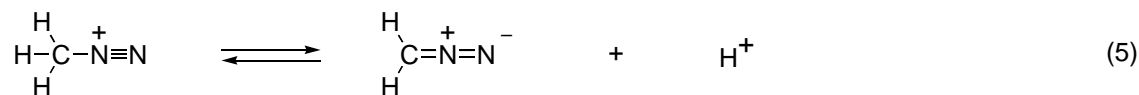
In contrast, the pK_a values of diazonium ions derived from diazoesters (**a**) and diazoketones (**b**) have been estimated to be between -5 and -2, respectively.[15] This is

$$\underset{a}{\overset{\displaystyle RO-\overset{\displaystyle O}{\overset{\|}{C}}}{\underset{\underset{H}{|}}{H-C-\overset{+}{N}\equiv N}}} \qquad \underset{b}{\overset{\displaystyle R-\overset{\displaystyle O}{\overset{\|}{C}}}{\underset{\underset{H}{|}}{H-C-\overset{+}{N}\equiv N}}}$$
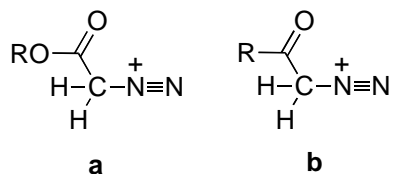
consistent with the much greater stability of diazoesters and diazoketones toward acid-promoted decomposition. So, various transition metals have been developed as diazo decomposition catalysts to afford more efficient reactivity in diazo decomposition reactions.

1.3.1 Mechanism of catalytic diazo decomposition. Metal carbene generation and reactions

Transition metal complexes that are effective catalysts for diazo decomposition are Lewis acids.[13] Their catalytic activity depends on coordinative unsaturation at the

metal center, which allows them to react as electrophiles with diazo compounds.[7] In the generally accepted mechanism for catalytic decomposition of diazo compounds (Scheme 2),[13,16-19] electrophilic addition causes the loss of dinitrogen and production of a metal-stabilized carbene (**14**). Transfer of the electrophilic carbene entity to an electron-rich substrate (S:) regenerates the catalytically active L_nM and completes the catalytic cycle.

$$SCR_2 \qquad S:$$

$$L_nM \qquad\qquad L_nM=CR_2$$
$$\mathbf{14}$$

$$R_2C=N_2 \qquad L_n\bar{M}-CR_2 \qquad N_2$$
$$+N_2$$
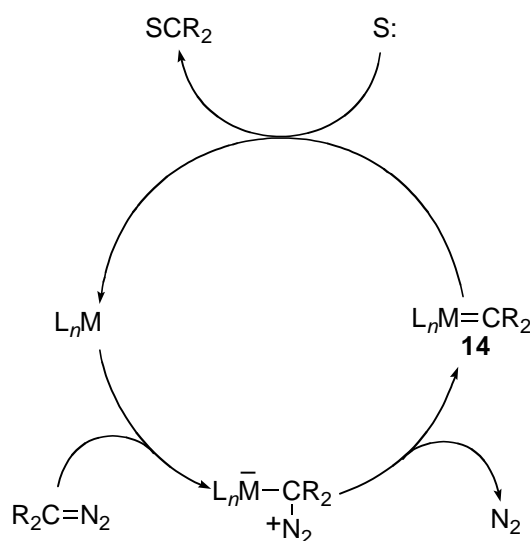
Scheme 2

The activities of catalytically active transition metal compounds towards diazo decomposition are dependent on both the electrophilicity of the transition metal compound and on the stability of the diazo compound.[15] Among diazocarbonyl compounds, those with two carbonyl groups flanking the diazo-bearing carbon are more stable toward transition metal-catalyzed decomposition than those with only one

7

carbonyl group.[17] Diazoesters are generally more stable than diazoketones, and diazoamides are more stable than diazoesters. This profile is a useful guide to determining the reaction conditions required to generate a metal carbene. For example, diazoacetoacetates and diazomalonates require higher temperatures for reactions with transition metal catalysts than do diazoacetates, which can undergo catalytic nitrogen loss at or below room temperature.[15]

Increasing stability

Z,Y = R, OR, NR$_2$
R, R' = alkyl, aryl, H

Increasing reactivity
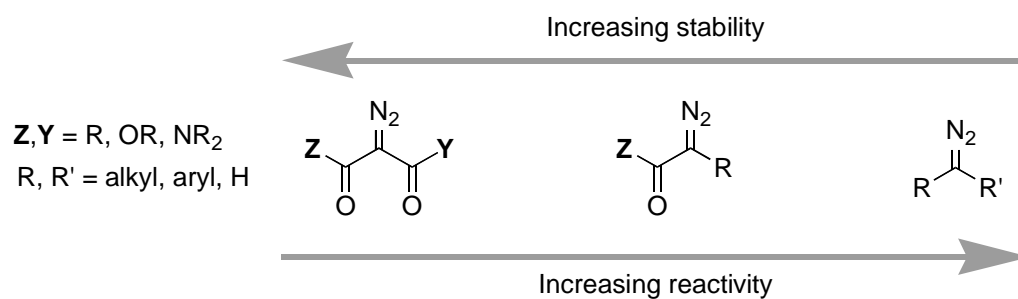
1.3.2 Rhodium catalysts for diazo decomposition

Dirhodium(II) catalysts are the most effective and versatile for diazo decomposition.[7,16-20] Dirhodium(II) tetraacetate (**15**) was first introduced by Teyssié and

15 **16** **17**
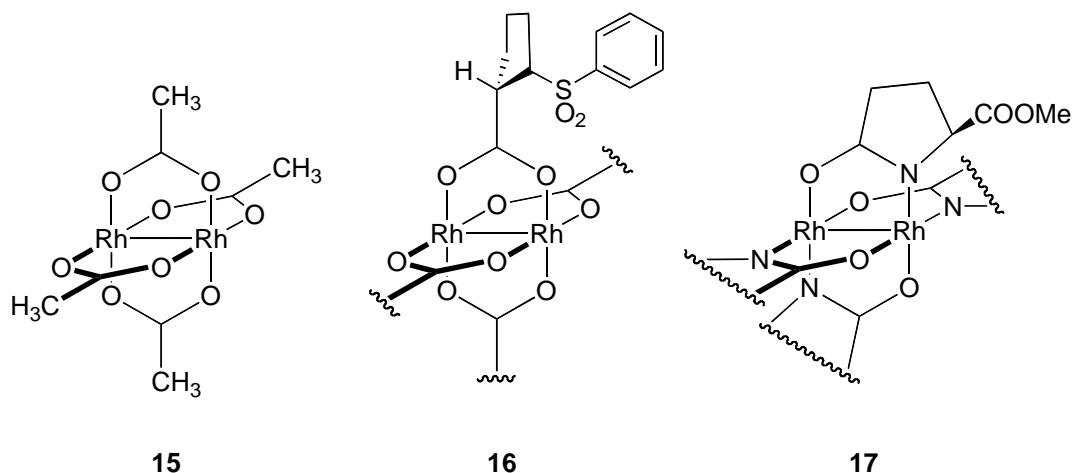
co-workers in 1973. Control of reactivity and selectivity in such catalysts can be
provided by varying the catalysts' bridging carboxylate (e.g. **16**[21]) or carboxamide (e.g.
17[22]) ligands (in the structures above, the ligand shown is repeated three more times).
Rhodium acetate **15** was originally employed as a catalyst for diazo decomposition in the
presence of aniline (eq. 6), namely, insertion of a metal-carbene into an N-H bond. The
reaction afforded the desired product **18** in 70% yield.[23] Compared to copper catalyst
with much lower yield (<30% usually),[24] the dirhodium catalyst offers the advantages of
mild conditions and higher yield.

18, 70%

9
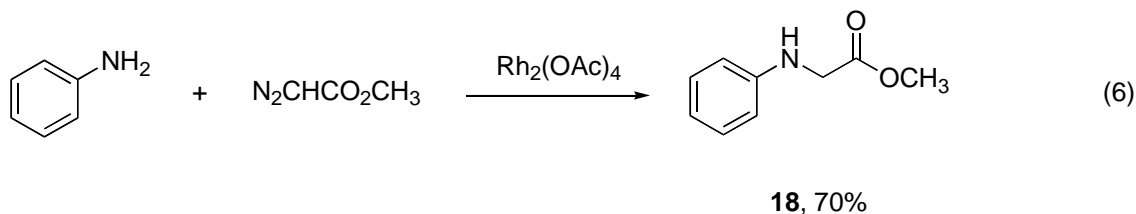
1.4 N-H insertion

Metal carbenes derived from α-diazocarbonyl compounds, e.g. **19**, are highly electrophilic. They readily react with an available Lewis base (B:) to form a zwitterionic adduct (Scheme 3, in which B: is PhNH$_2$). Catalytically generated electrophilic metal

19
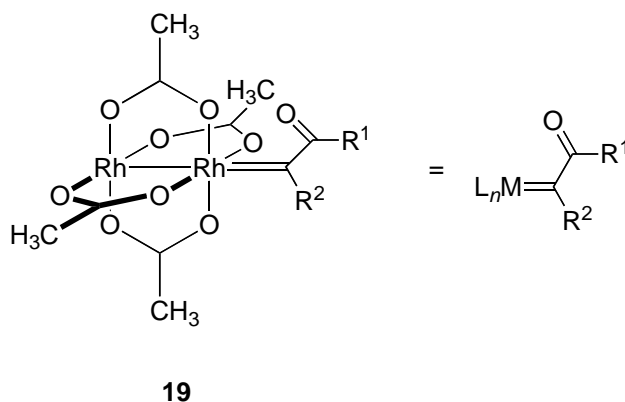
carbenes add to Lewis bases, characteristically heteroatom-substituted organic compounds, to form zwitterionic adducts **20,** which can either dissociate to form rearranged products (or form a "free" ylide) and the catalyst, or revert to the metal carbene and Lewis base. With catalytically generated metal carbenes, especially those of rhodium, the metal-carbon bond of the intermediate metal-stabilized ylide is generally weaker than the R$_2$C-base bond, and the preferred cleavage is that of the metal-carbon bond. The ease with which catalytically generated metal carbenes transfer the carbene entity to a heteroatom of an organic base is the basis for the synthetic utility to this diazo decomposition methodology.[7]
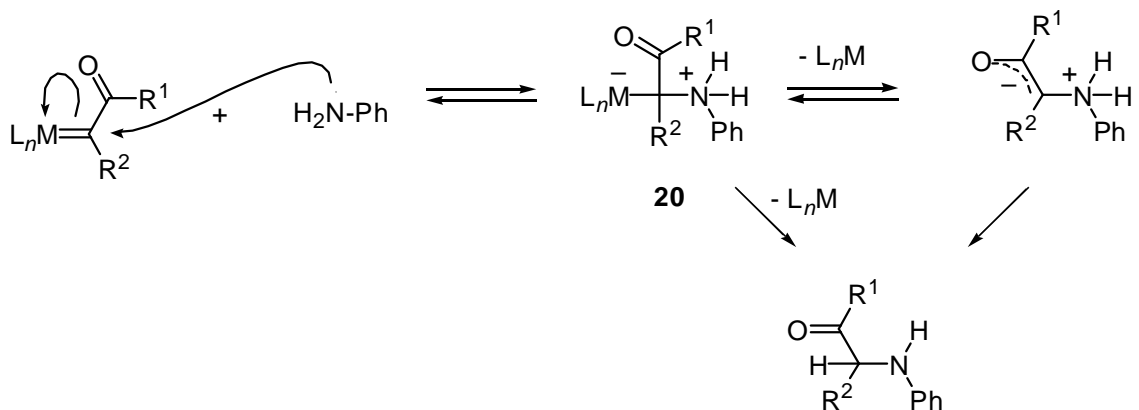
Scheme 3

1.4.1 Intermolecular N-H Reaction

Insertion into N-H bonds by diazocarbonyl compounds attracted little attention as a synthetic route to α-amino ketones or esters until 1978, when a bicyclic β-lactam synthesis was published from the Merck laboratories.[25-27] Since then the power of this reaction has been demonstrated dramatically, especially the intramolecular reaction leading to nitrogen heterocycles. As mentioned, the introduction of rhodium(II) catalysts for N-H insertion led to major improvements with reaction between EDA and aniline in the presence of rhodium(II) acetate furnishing in 70% yield the insertion product (eq. 6).[28]

Reactions are carried out either neat or in solution (benzene or ethylene glycol dimethyl ether). In a similar fashion, Landais and Planchenault[29] used rhodium(II) acetate in benzene to bring about N-H insertion of aniline in an allylic amino ester

synthesis (eq. 7).

(7)

68%
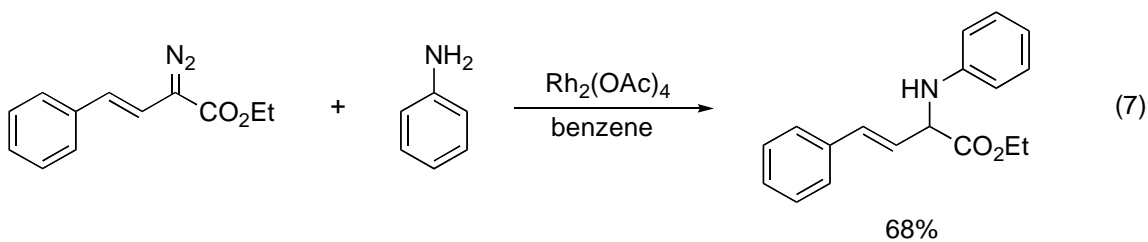
N-H insertion with diazocarbonyl compounds is not limited to amino functions. Insertion reactions involving amides, β-lactams, and carbamates are also known. Some examples are shown in eqs. 8,[30] 9,[31] and 10.[30] For the reaction in eq. 10 two different

(8)

81%

(9)

(= Cbz-NH₂)

85%

(10)

71%
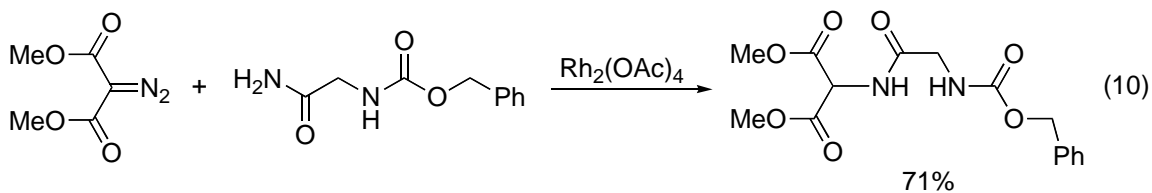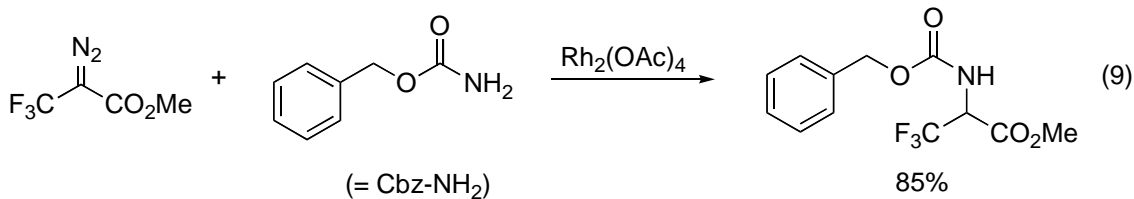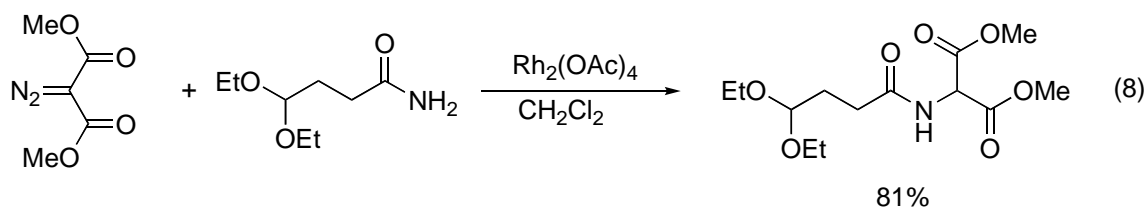
N-H sites are available, one in the form of an amide and the other a carbamate. The former is preferred.

1.4.2 Intramolecular N-H Reaction

By far the most successful metal-catalyzed N-H insertion reactions have been intramolecular, leading to nitrogen heterocycles. Most recent studies, mainly by Rapoport and co-workers,[32] have established that while five-membered formation is preferred kinetically in the intramolecular insertion, it is possible to construct four- to six-membered aza rings from simple, conformationally mobile acyclic diazoester precursors. Rhodium(II) acetate was used as catalyst throughout, and variations in solvent, temperature, and catalyst concentration were found to play a role in determining product distributions. A summary of the results is shown in Scheme 4. Cyclization to four- and five-membered rings containing N occurred efficiently and selectively (entries 1 and 2). With the diazo compound in entry 3, the opportunity exists for both intramolecular C-H and N-H insertion. Finally, the diazo compound in entry 4 presented the option of five- and six-membered ring formation from C-H insertion and seven-membered heterocycle formation from N-H insertion. Thus the kinetic preference for five-membered ring formation completely overwhelms any tendency for N-H insertion. However, four-membered rings are also directly accessible with rhodium(II) catalysts.[33]
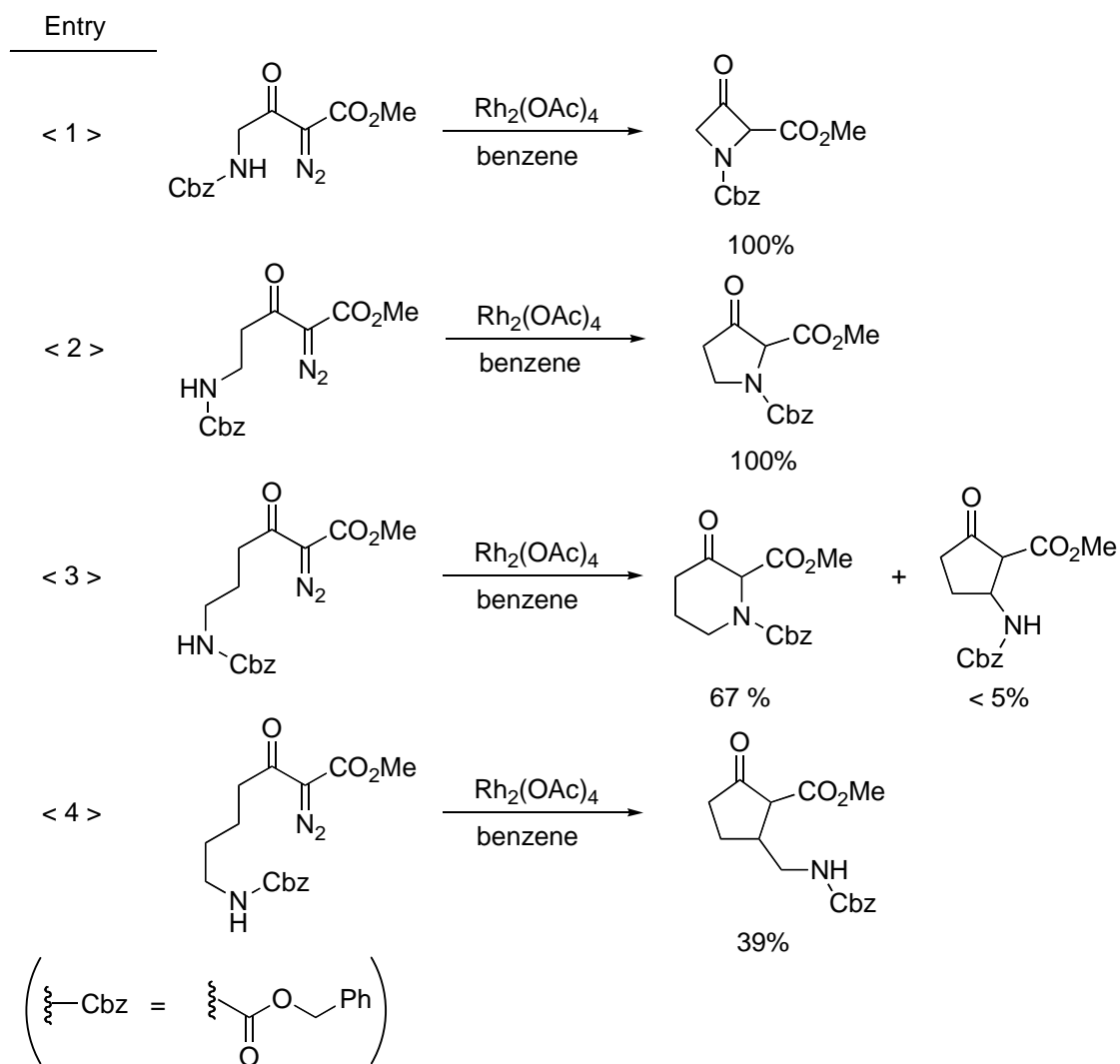
Scheme 4

Seebach[34] and McKervey[35] and their collaborators have found that Boc- and Cbz-protected α-aminodiazoketones derived from L-alanine, L-valine, and L-phenylalanine cyclize very efficiently to the azetidin-3-one derivatives (eq. 11).

(11)

PG = Boc, Cbz
R = Me, *i*-Pr, PhCH$_2$

50 - 60%
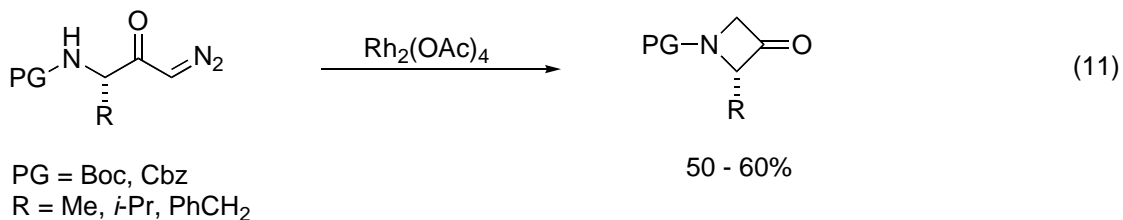
1.5 Bisdiazo compounds

The decomposition of bisdiazo compounds in rhodium(II) catalyst using in the synthesis is limited studied. Recently, the photochemistry of bisdiazo compounds was studied for the synthesis of highly strained compounds (eq. 12).[36]

(12)
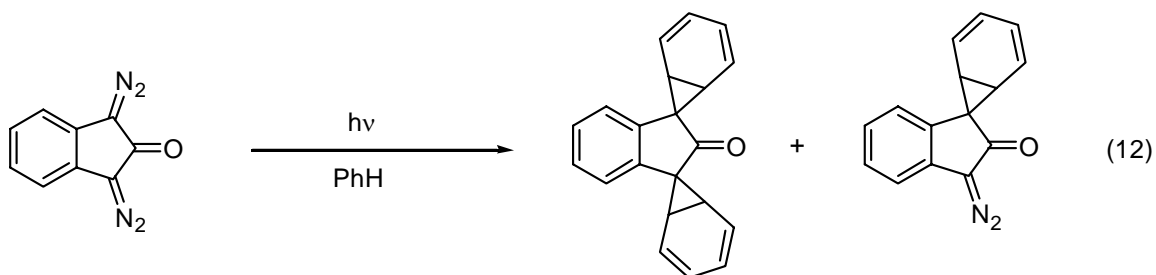
Also, the intramolecular insertion reaction of bisdiazo compounds was established as a useful route to cyclic ethers, especially some medium-ring and large-ring compounds. Kulkowit and McKervey used Cu(II)(acac)$_2$ in benzene to catalyze the intramolecular O-H insertion reaction of a bisdiazo ketone (eq. 13).[37]

$$m = 6, n = 1, 27\% \text{ yield}$$
$$m = 8, n = 3, 62\% \text{ yield}$$
$$m = 9, n = 3, 21\% \text{ yield}$$
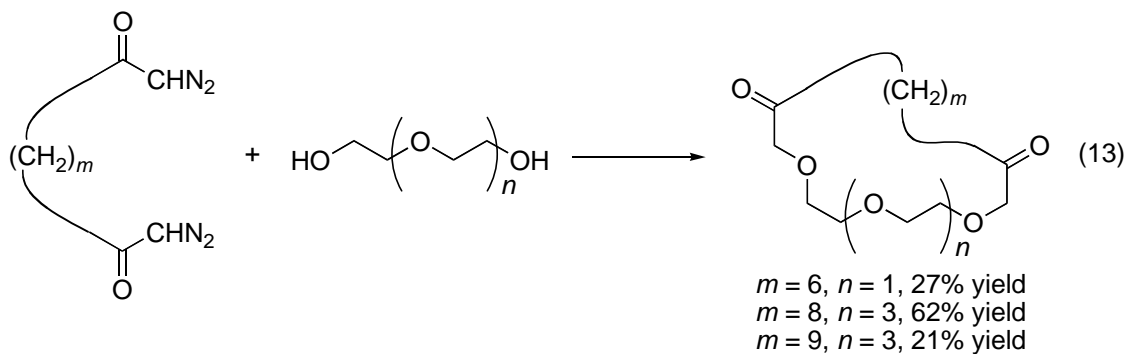
1.6 Diamino Dicarboxylic Acids

Amino acid research is a large and important field. Diamino dicarboxylic acids or bis(amino acid)s are characterized by two glycine residues that are connected by a spacer via the α-carbons. They contain two asymmetric carbons, two chemically identical amino
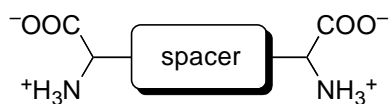
a bis(amino acid)

and carboxylic groups. This character confers on bis(amino acid)s an important role in studying biosynthesis inhibitors, such as investigating the synergistic effect when bacterial infections result in an immune response.[38] For example, bacterial peptidoglycan (Scheme 5) is a giant macromolecule consisting of linear heteroglycan chains cross-linked by short peptide chains. When studying the synergistic effect, pure muramyl peptides with different lengths of peptide chain are required. The bis(amino acid)s then

16

function as cross-linkers in the peptidoglycan network.

DAA = diamino acid or L-lysine

(AA)$_n$ = n amino acids, with n = 0 - 5
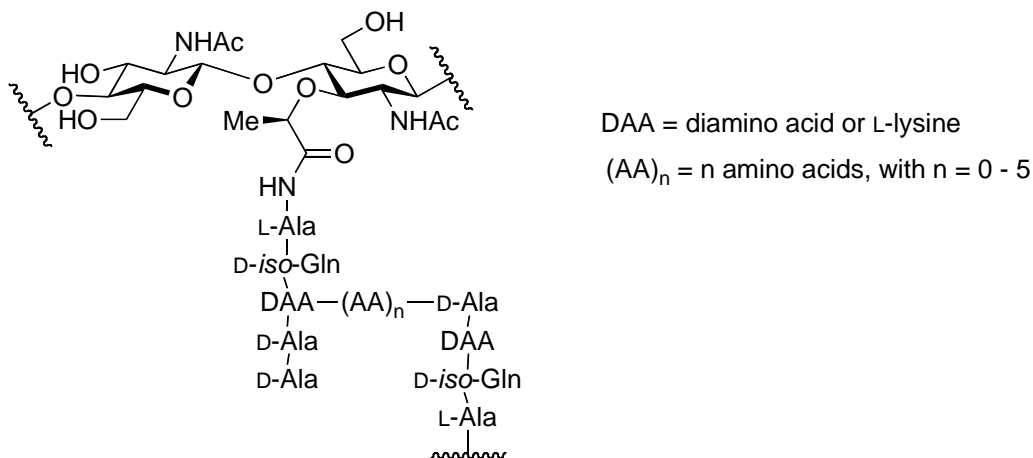
Scheme 5

Also, the use of diamino dicarboxylic acid derivatives for peptidomimetic drug design is becoming more commonplace.[39] Recently, members of this class have been used as conformational constraints in order to mimic the secondary structures of peptides, such as β-turns,[40] and to stabilize a helical conformation.[41] As most peptides are flexible and have many conformations in solution which is difficult to determine the activity of the peptide. The conformational constraints may be helpful in elucidating these structures by restricting the peptide to a particular conformation or closely related family of conformations.[42] After being bridged or linked by a bis(amino acid), the peptide will be restricted to a particular conformation which will be associated with a receptor and a desired biological effect can be obtained (Scheme 6).[45(a)]

17
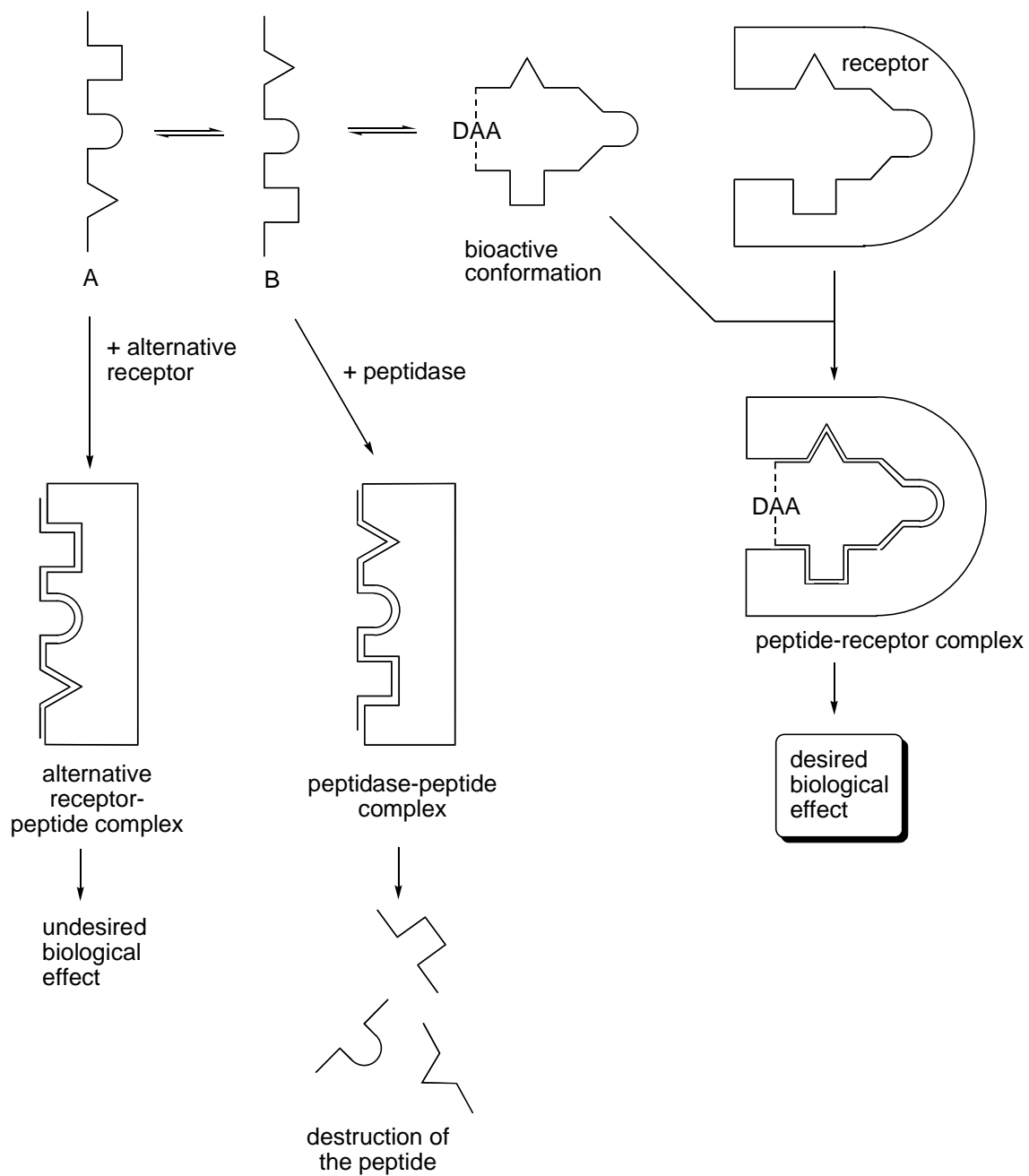
Scheme 6

1.7 Diaminoglutaric Acid and Its 3-Substituted Derivatives

Recently, much interest has been focused on the synthesis of unnatural and

unusual α-amino acids,[43] since this class of compounds has an intrinsic biological activity. Such compounds can also modify biological potency and improve metabolic stability in a useful way when incorporated into medicinally important peptides.[44] Meanwhile, the synthesis of the modified peptides based on the substitution of α-amino acids by non-standard residues in order to control flexibility and to determine conformations or to change the bioavailability and the inhibitory activity of the peptide has attracted significant attention.[43(b),44,45] In particular, the incorporation of α-amino acids with a functional group that can act as a receptor ligand is of great interest.

1.7.1 Diaminoglutaric Acid

Glutaric acid is an important chemical messenger which is released in most of the excitatory synapses of mammalian central nervous systems.[46] Several syntheses of differentially functionalized (2*R*,4*S*)- and (2*R*,4*R*)-diaminoglutaric acids (DAG) **21** and **22** which was employed as a building block for peptidomimetics have been reported.[47]

21   **22**

Scheme 7[47(d)] and Scheme 8[47(f)] summarize two reported routes to **21** and **22**.
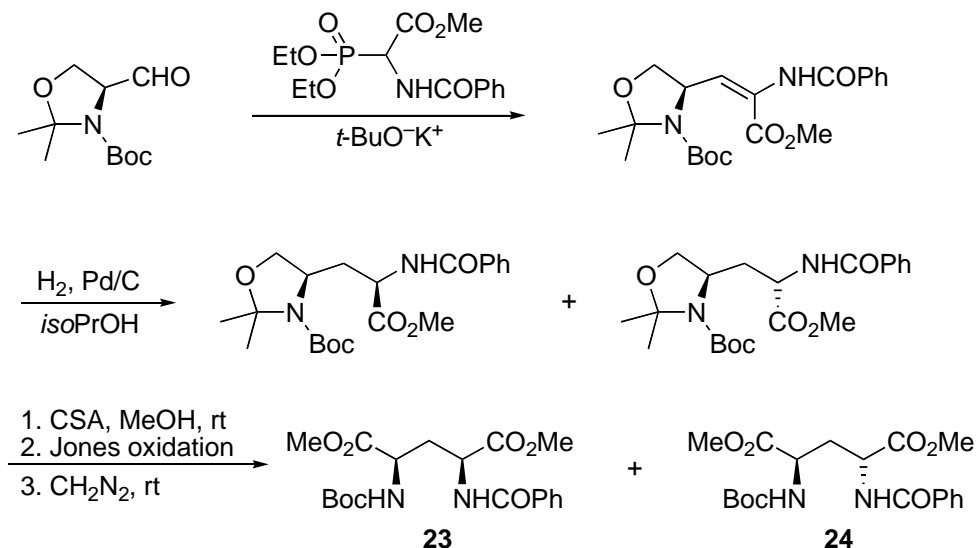
Scheme 7

CSA = camphorsulfonic acid
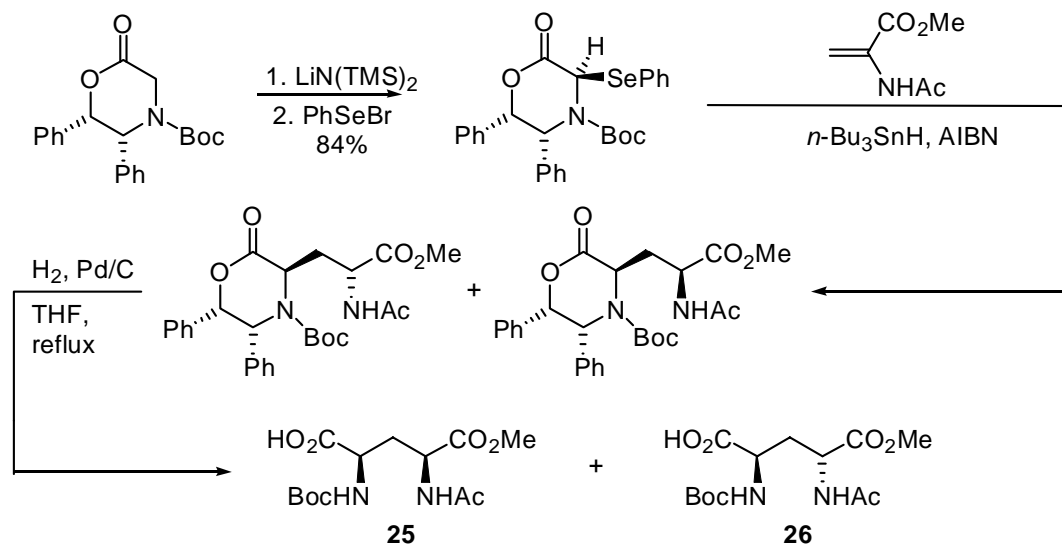
Scheme 8

The full syntheses are moderately lengthy. In work leading to his Ph. D. degree,

Dr. Minmin Yang of our laboratory discovered that the N-H insertion reaction of diethyl

2-diazoglutaconate was accompanied by a shift of the double bond (Scheme 9). This

created the possibility for another diazotization/N-H insertion sequence. The net result was a concise high-yield synthesis of a bis(amino acid) derivative. When the final reduction was a hydrogenation over a chiral catalyst, partial control of stereochemistry was afforded.[47(g)]
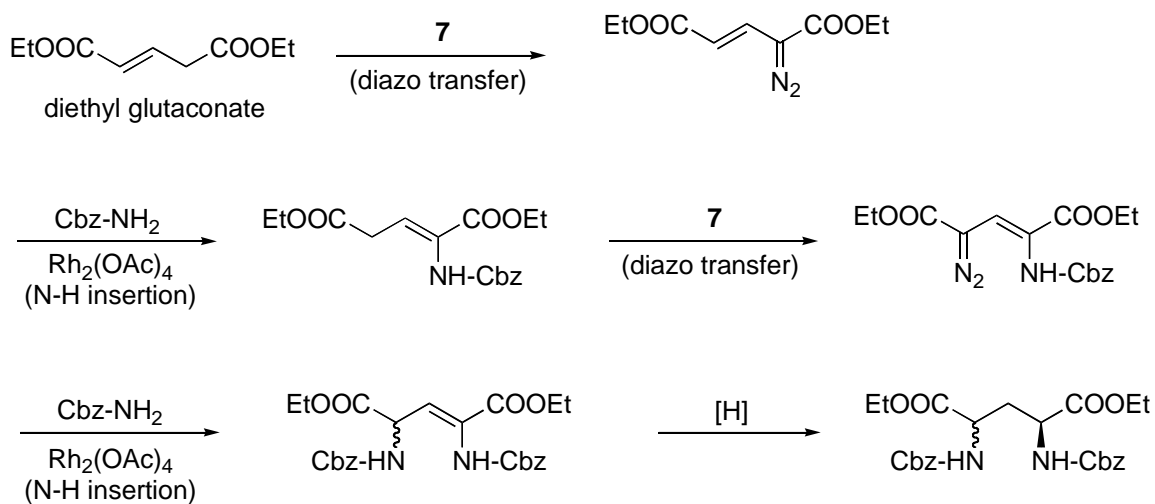
Scheme 9

1.7.2. 3-Substituted Diaminoglutaric Acids

The incorporation of α-amino acids with a functional group that can act as a receptor ligand, such as 3-substituted diaminoglutaric acids, has attracted interest as possible peptidomimetics. Our target **27** here is to introduce fluorine into the β–position of diaminoglutaric acid.

F

MeOOC ⟋ ⟍ COOMe

Cbz-HN   NH-Cbz
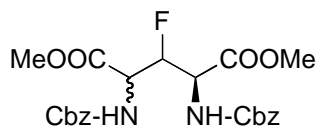
27

It has been known for some time that fluorine can have profound and unexpected results on biological activity.[48] Once introduced, the high carbon-fluorine bond energy renders the substituent relatively resistant to metabolic transformations. The electronegativity of fluorine can have pronounced effects on the electron distribution in the molecule, affecting the basicity or acidity of neighboring groups, dipole moments within the molecule and the overall reactivity and stability of neighboring functional groups. As a consequence of the available electron density, fluorine can function as a hydrogen bond acceptor.[49] Introduction of fluorine can be carried out successfully in the presence of various functional groups using diethylaminosulfur trifluoride (DAST) as a fluorodehydroxylation reagent (Scheme 10).[50]
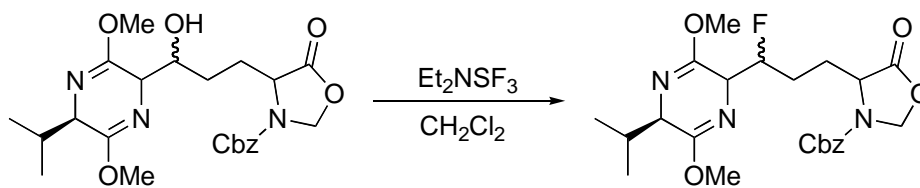
Scheme 10

We propose that the fluorine of **27** could be introduced this way (Scheme 11).

F
MeOOC COOMe ⟹ MeOOC COOMe
Cbz-HN NH-Cbz Cbz-HN NH-Cbz
27 **28**

OH
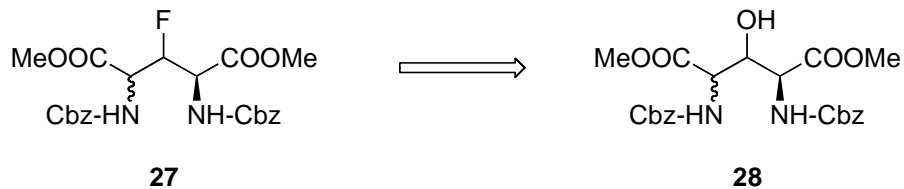
Scheme 11

The importance of enzymatic decarboxylations of amino acids in biosynthetic pathways suggested the utility of specific inhibitors of the decarboxylation enzymes in studying these pathways.[49] Fluoroacylated amino acids have been recognized as potent suicide inhibitors of enzymatic decarboxylation reactions.[51] The enzymatic inactivation is thought to be dependent upon loss of fluoride from the intermediate base **29** formed between pyridoxal phosphate and the fluoroacyl amino acid. Loss of fluoride generates a reactive acceptor **30** which can add an enzyme bound nucleophilic functional group. The covalently bound enzyme **31** is no longer free to bind additional substrate (Scheme 12). This character gives the fluoro-substituted amino acids high biological potential to serve as inhibitors to disrupt polyamine synthesis, with important implications for various anti-biological agents.[49]

A short and easy synthesis route to our target compound **27** starting from cheap and commercial available compound **32** was developed as briefly shown in Scheme 13. The novel aspect of this proposed route is the use of bisdiazo compound **33** to introduce both amino nitrogens simultaneously by double N-H insertion.
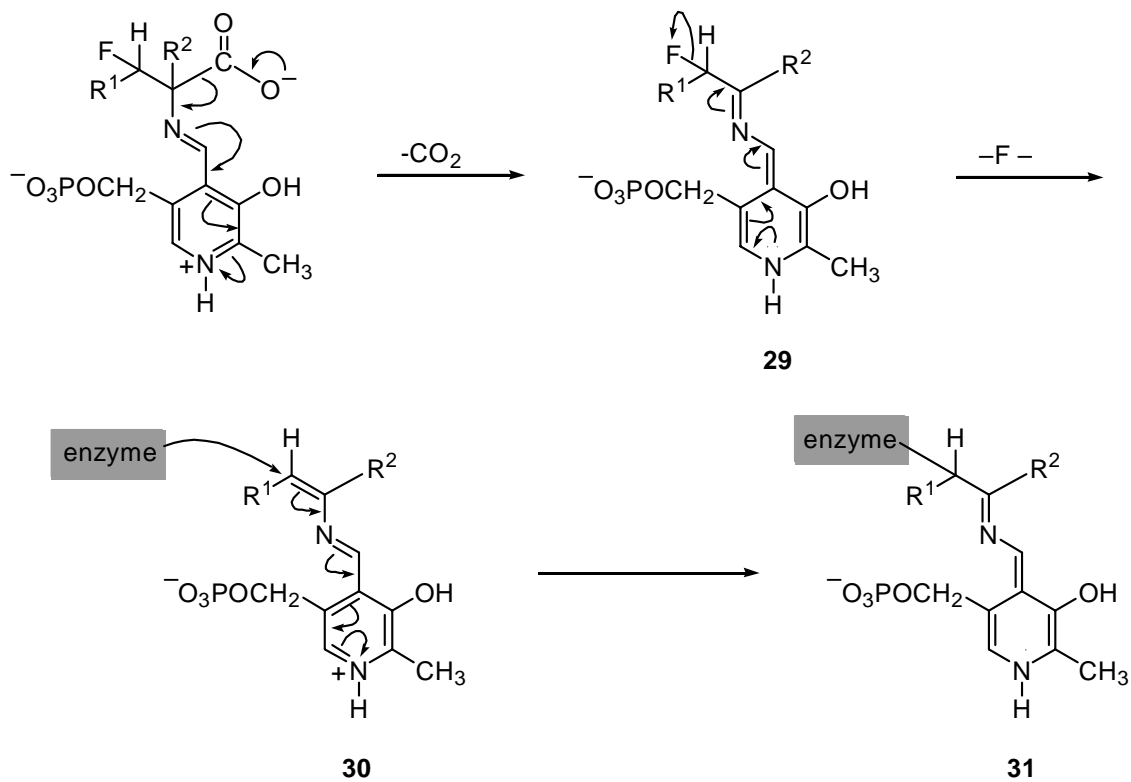
Scheme 12
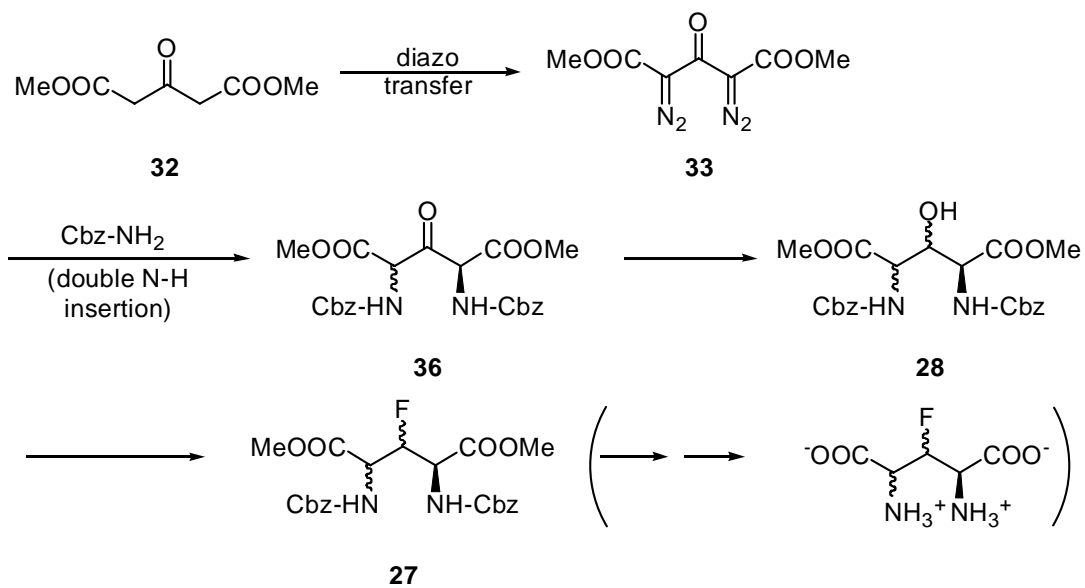
Scheme 13

2. PART I. RESULTS AND DISCUSSION

2.1. Synthesis of Bisdiazocarbonyl Compounds.

The bisdiazocarbonyl compound could be synthesized by diazo transfer from sulfonyl azide **7**.[52] Dropwise addition of aqueous sodium azide to a stirred solution of *p*-acetoamidobenzenesulfonyl chloride **13** in methylene chloride containing tetrabutyl-ammonium bromide (TBAB) at 0 °C, gave *p*-acetoamidobenzenesulfonyl azide (*p*-ABSA) **7**,[53] as colorless crystals in 91.3% yield.

$$SO_2Cl \quad + \quad NaN_3 \quad \xrightarrow[\text{CH}_2\text{Cl}_2]{(\textit{n}\text{-Bu})_4\text{N}^+\ \text{Br}^-} \quad SO_2N_3 \qquad (14)$$

13   **7**, 91%
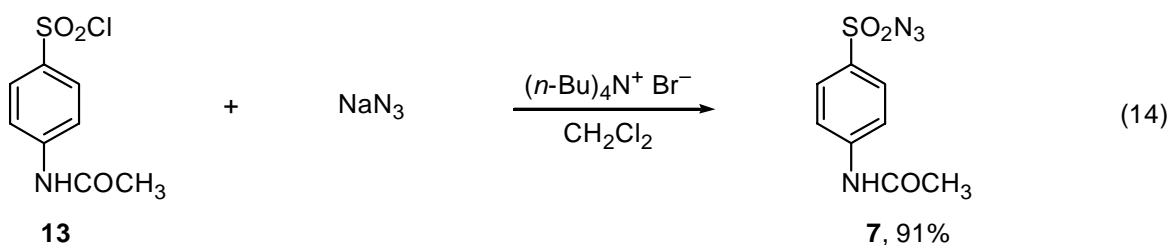
Compound **7** in acetonitrile was added dropwise to an acetonitrile solution of dimethyl 3-oxoglutarate **32** and triethylamine at 0 °C, in hopes of preparing **33** (eq. 14).

$$SO_2N_3 \quad + \quad MeOOC \diagdown \overset{O}{\diagup} \diagdown COOMe \quad \xrightarrow[\text{CH}_3\text{CN}]{\text{Et}_3\text{N}} \quad MeOOC \overset{O}{\diagup} \underset{N_2 \quad N_2}{\diagdown} COOMe \qquad (15)$$

7   **32**   **33**, 92%
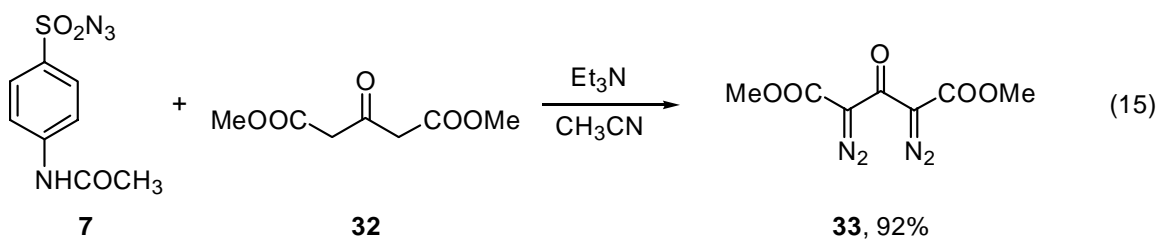
The resulting yellow oil showed only one methyl ester peak in its ^{1}H NMR spectrum (Figure 1). The peak at 74.2 ppm in the ^{13}C NMR spectrum (Figure 2), and the strong peak at 2133 cm^{-1} in the IR spectrum (Figure 3) indicated that the C=N=N moiety was present in **33**. Other peaks in the ^{13}C NMR spectrum can be reasonably assigned as follows: 52.8 ppm, -CH$_3$; 161.4 ppm, ester carbonyls; 174.5 ppm, ketone carbonyl.
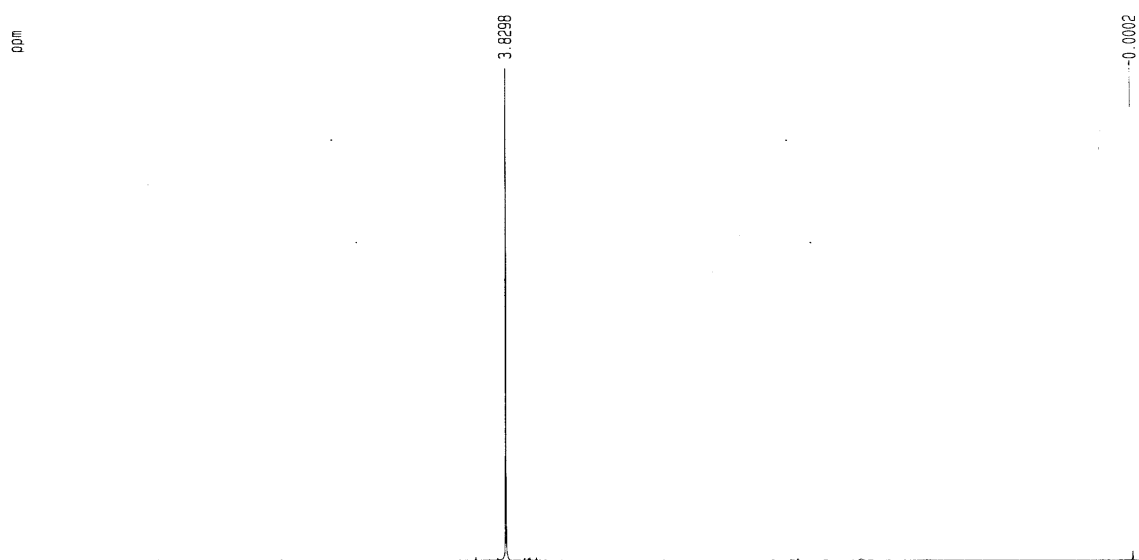
Figure 1. [1]H spectrum of compound **33**

A possible reaction product, **34**, is inconsistent with the IR results. It is also ruled out by the results of elemental analysis (calcd for C$_7$H$_6$N$_4$O$_5$ (**33**) %C, 37.18; %H, 2.67; %N 24.77: found %C, 37.15; %H, 2.69; %N, 24.53).

34
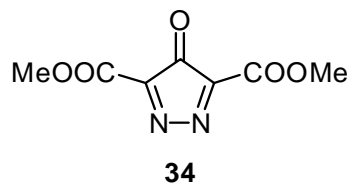
Thus the diazo transfer reaction afforded the hitherto unknown compound dimethyl 2,4-bis(diazo)-3-oxoglutarate **33** in excellent yield. (eq 15).

C13 CDC13

ppm 174.505 161.436 77.548 77.433 77.229 76.911 74.247 52.757
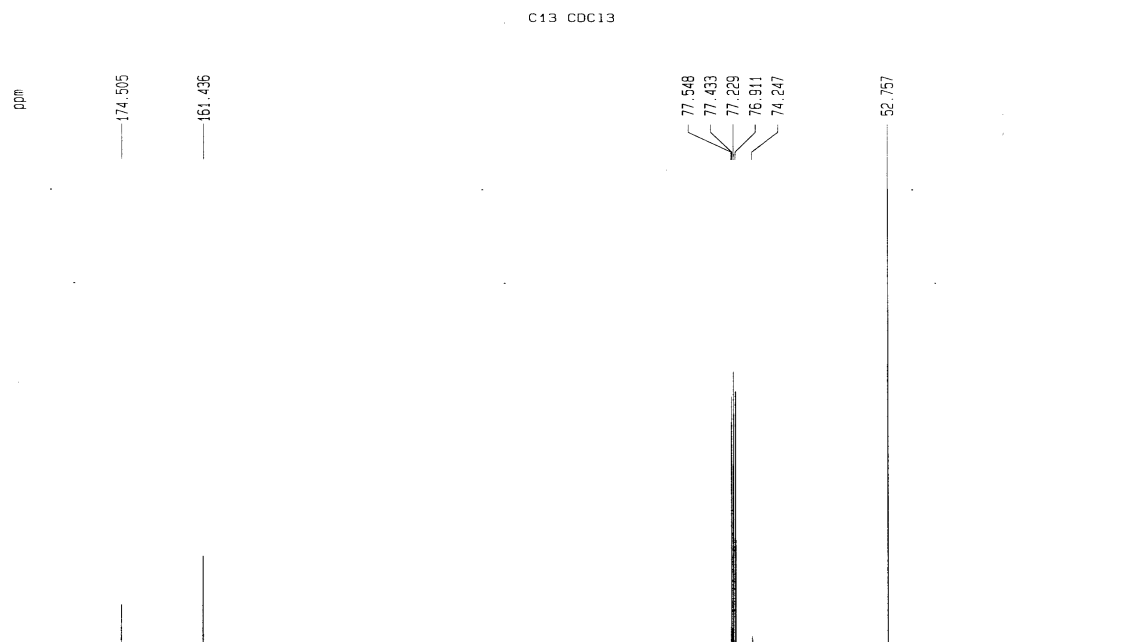
Figure 2. ^{13}C spectrum of compound **33**

dimethyl diazo

3004.61
2955.96
2133.32
1719.05
1601.23
1433.92
1321.45
1192.27
1126.22
996.13
885.3
850.34
834.54
807.74
785.51
750.08
763.07
698.88

%Transmittance

Wavenumbers (cm-1)
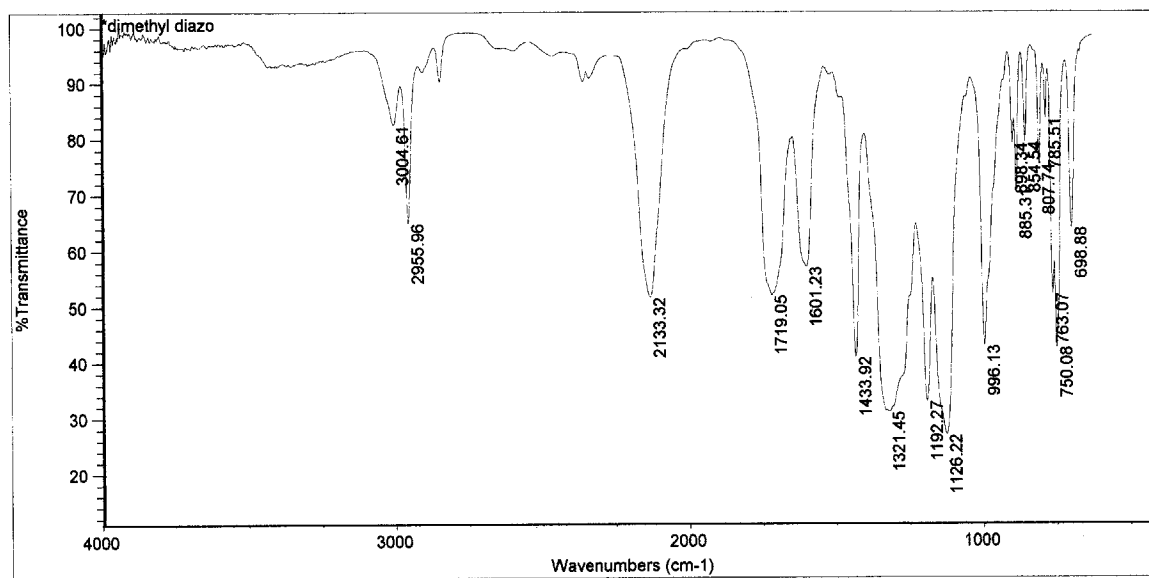
Figure 3. IR spectrum of compound **33**

27

2.2. N-H insertion of Rh(II)-stabilized carbenoid from bis(diazo) compound 33 into Cbz-NH₂.

Benzyl carbamate (Cbz-NH$_2$) **35**, which was required for the N-H insertion reaction of dimethyl 2,4-bis(diazo)-3-oxoglutarate **33**, was easily afforded by bubbling dry ammonia gas through a methylene chloride solution of benzyl chloroformate at 0 °C (eq 16).

$$\text{(16)}$$
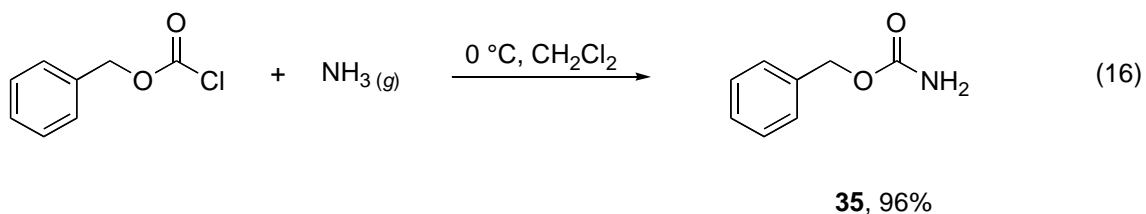
Dimethyl 2,4-bis(diazo)-3-oxoglutarate **33** reacted with excess benzyl carbamate **35** in refluxing methylene chloride, catalyzed by Rh$_2$(OAc)$_4$ (eq 17). After the reaction solution had refluxed for 1 h, the TLC showed bis(diazo) compound **33** was consumed.

$$\text{(17)}$$
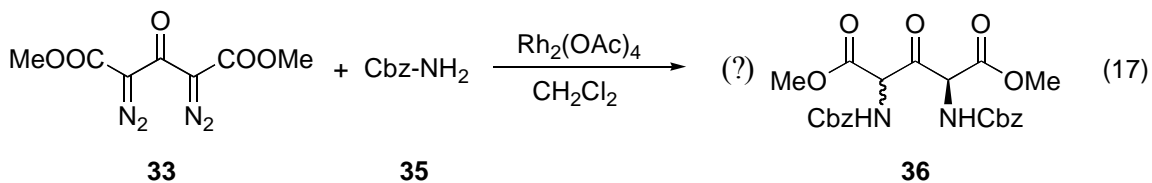
However, the purification of products was not smooth. The TLC exhibited a spot with a long tail when using 1:1 hexane:ethyl acetate as eluent. Trying various solvent systems,

28

such as methylene chloride with ethyl acetate, chloroform with methanol, and methylene chloride with toluene, did not solve the separation problem. Fortunately, when the reaction mixture was passed though a silica gel chromatography column eluted with 1:1 hexane:ethyl acetate, collecting all fractions before a yellow fraction on the column gave a mixture which could be separated by TLC using 5:1 hexane:ethyl acetate. Finally, a colorless oil was afforded by column chromatography in 63% yield. However, the ^{1}H NMR spectra (Figure 4) showed four single peaks from 3.67~3.75 ppm which indicated four kinds of methyl groups of the methyl ester. Initially, we thought that the separated colorless oil was still a mixture. However the use of various solvent systems to attempt to separate this oil by TLC failed. The M+1 peak indicated on mass spectrum and elemental analysis of **36** were successful, which means the N-H insertion reaction occurred and the desired product was formed. Why did the NMR spectra show a mixture?

in CDCl3

ppm

3.75183
3.72855
3.71173
3.67097
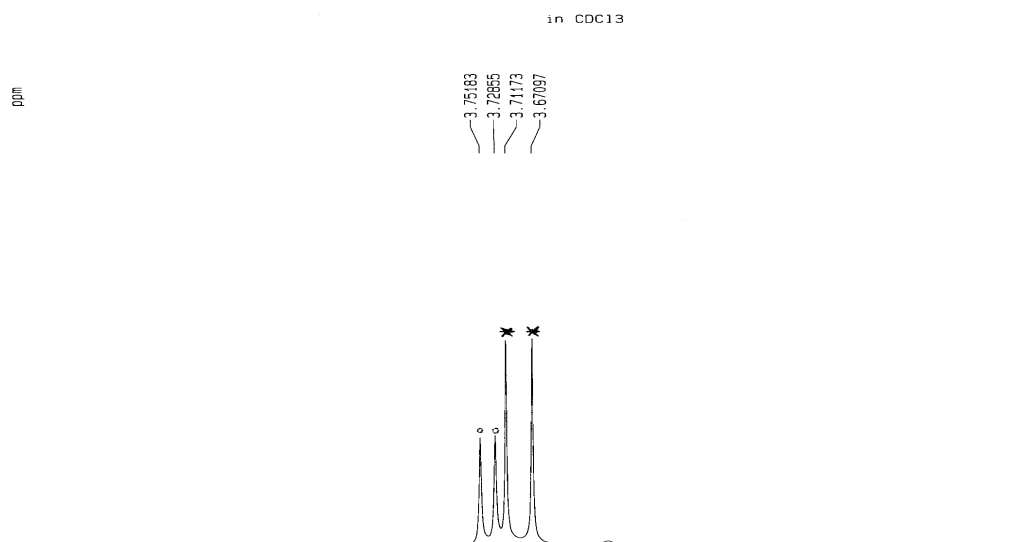
Figure 4a. Partial ^{1}H NMR spectrum of **36**: OCH$_3$ region.

29
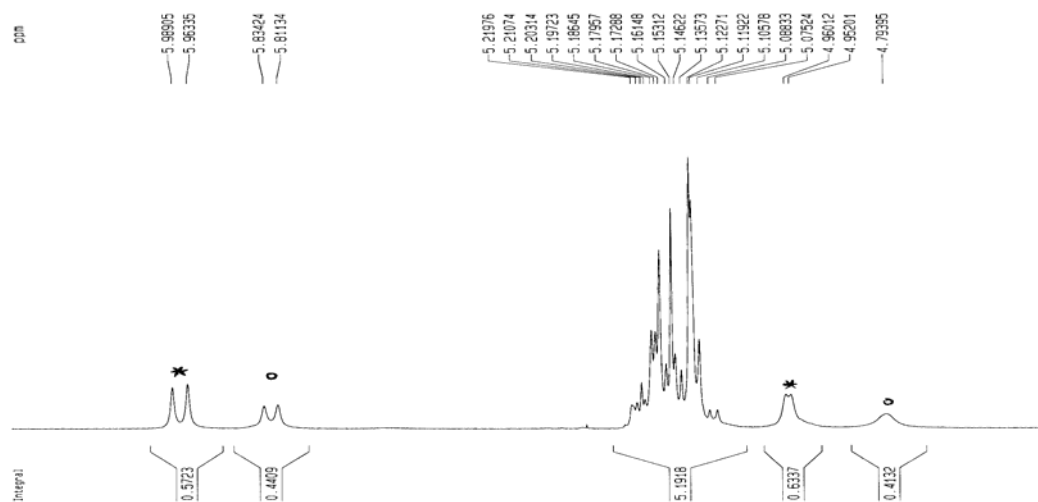
Figure 4b. Partial ^{1}H NMR spectrum of **36**: 4.7 ~ 6.0 ppm region.
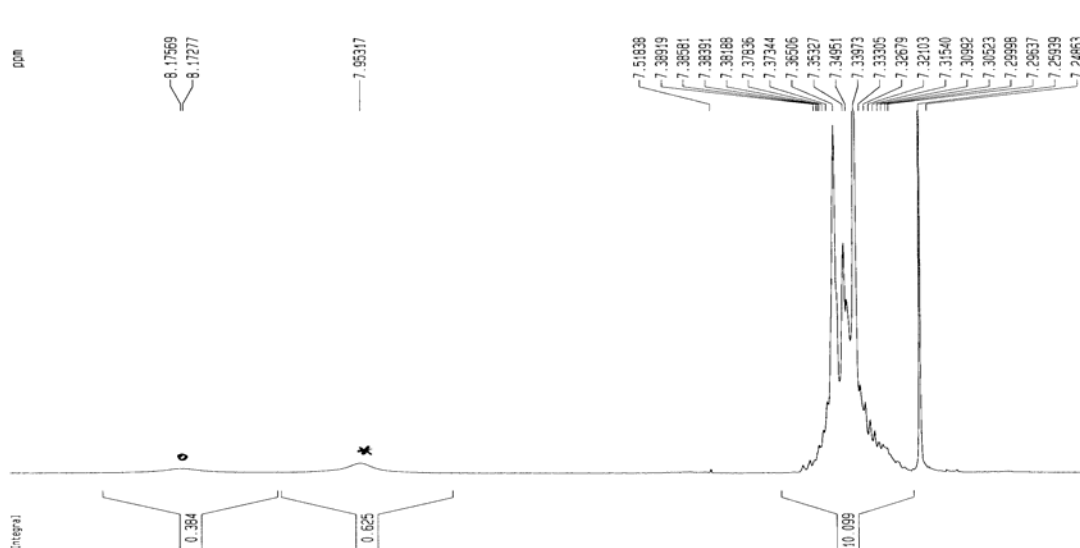
Figure 4c. Partial ^{1}H NMR spectrum of **36**: 7.0 ~ 8.2 ppm region.

It is reasonable to assume that compound **36** is highly enolic (Scheme 14). In Scheme 14, the carbons are numbered only to distinguish one end of the molecule from the other. That is, the enol double bond might be between C2 and C3, which we denote with a suffix **"a"**, or it might be between C3 and C4, which we denote with a suffix **"b"**.

30

Furthermore, geometrical (*i.e.* cis-trans) isomerism is possible for these enols. Thus, as
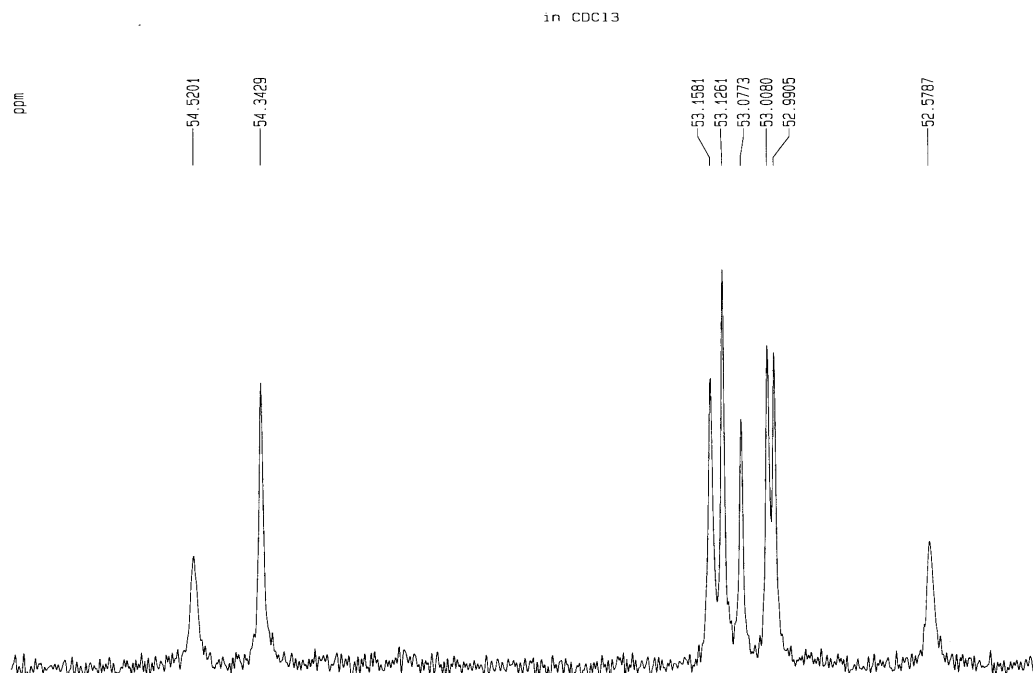
Figure 5a. Partial ^{13}C NMR spectrum of **36**: 52.5 ~ 54.6 ppm region. A DEPT-135

experiment showed all these peaks were from CH$_3$/CH carbons.
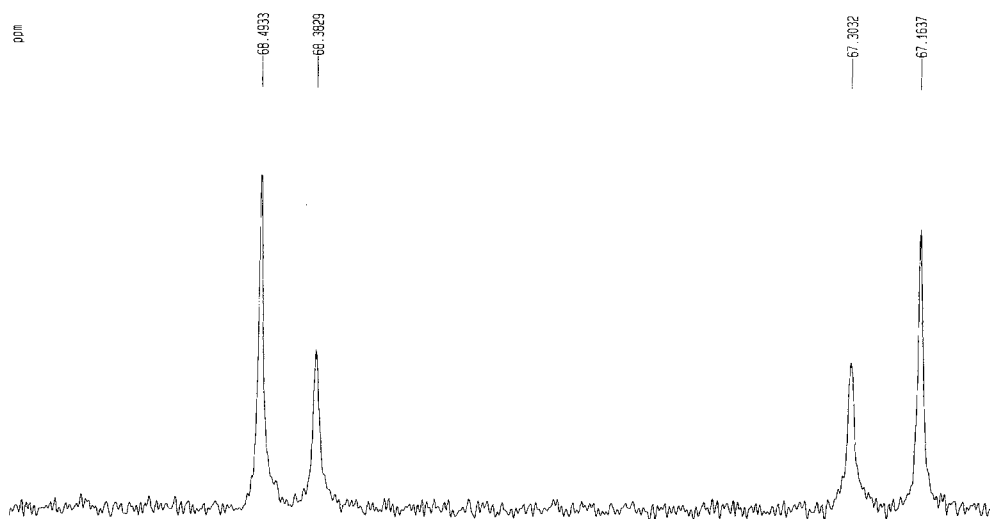
Figure 5b. Partial ^{13}C NMR spectrum of **36**: 67.1 ~ 68.4 ppm region. A DEPT-135

experiment showed all these peaks were from CH$_2$ carbons.

31
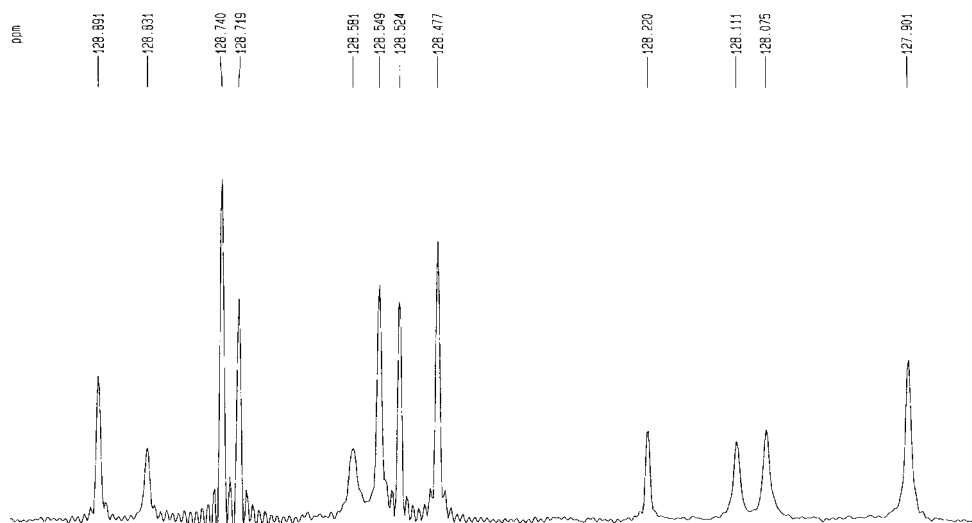
Figure 5c. Partial ^{13}C NMR spectrum of **36**: 127.9 ~ 128.9 ppm region. A DEPT-135

experiment showed all these peaks were from CH$_3$/CH carbons.
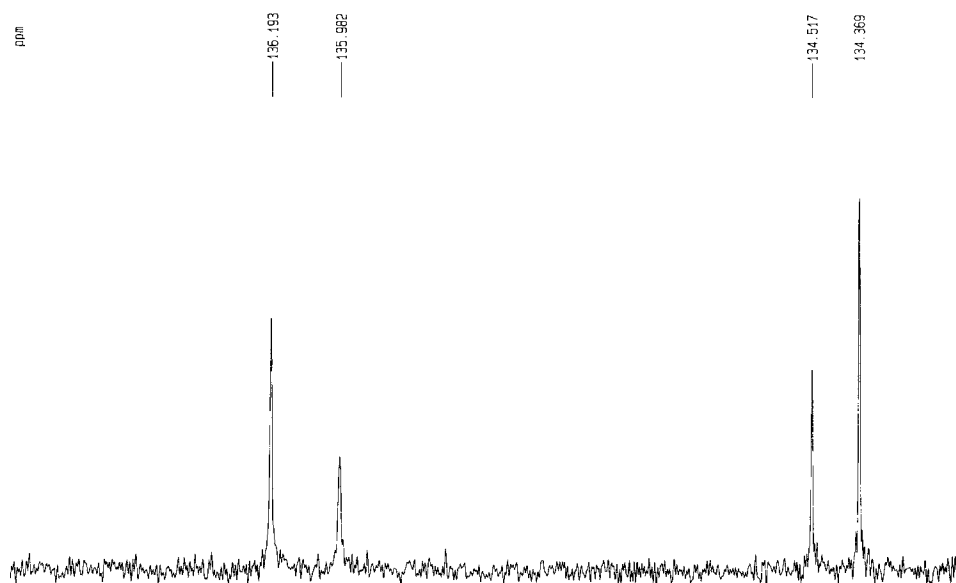
Figure 5d. Partial ^{13}C NMR spectrum of **36**: 134.3 ~ 136.2 ppm region. A DEPT-135

experiment showed all these peaks were from quaternary carbons.
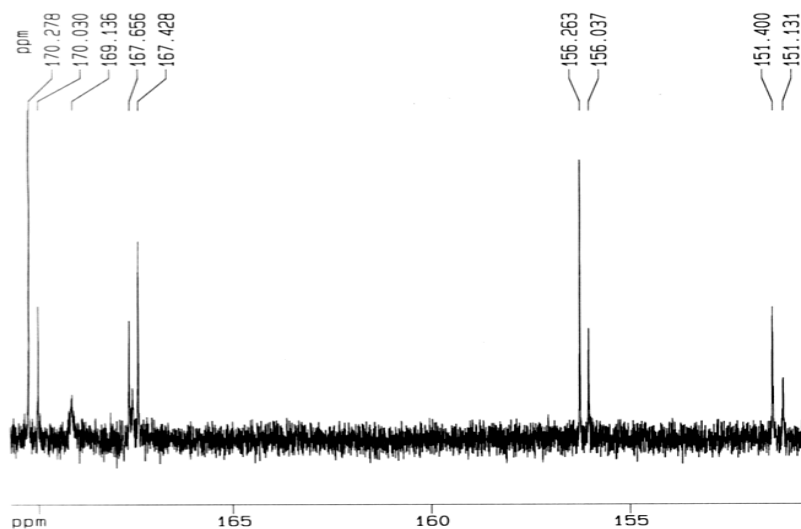
Figure 5e. Partial ^{13}C NMR spectrum of **36**: 151.1 ~ 170.3 ppm region. A DEPT-135

experiment showed all these peaks were from quaternary carbons.

shown in Scheme 14, we have four possible forms of **36**, namely *E*-**36a**, *E*-**36b**, *Z*-**36a**,

and *Z*-**36b**. This explains the four methyl signals in the 3.67 ~ 3.75 ppm region of the ^{1}H

NMR. In Figure 4a, two methyl signals are marked with ° and two with *. The two °

peaks are equal in area, as are the two * peaks. Since **"a"** forms and **"b"** forms are equal

in energy, $K_{eq} = 1$, *i.e.*, there must be equal amounts of *E*-**36a** and *E*-**36b**, and equal

Scheme 14
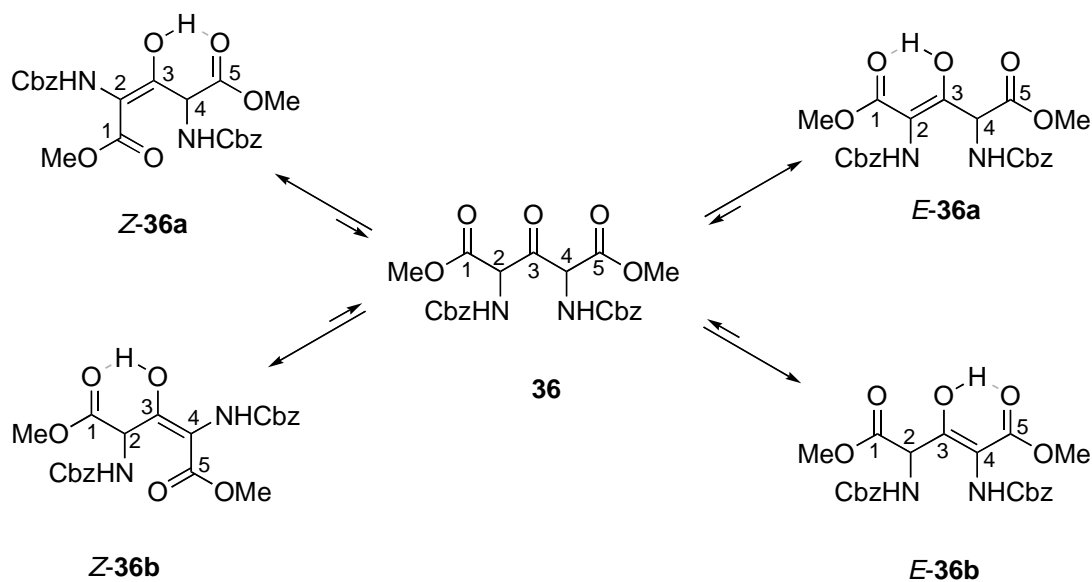
amounts of *Z*-**36a** and *Z*-**36b**. The **a** ⇌ **b** equilibrium in this solvent (CDCl₃) at ambient probe temperature is apparently slow on the 400 MHz NMR timescale, so separate signals for **a** and **b** forms are observed. However, there is no reason to expect *E* and *Z* isomers to be present in equal amounts. From integration of ° peaks versus * peaks we find a 60:40 ratio. It is reasonable to speculate that the more abundant form is the *E* form, because the internal hydrogen bond in the *E* isomer appears stronger than that in the *Z* form, making the *E* form slightly more stable.

To help assign the remainder of the peaks in the ¹H and ¹³C NMR spectra, model compound **37** was used.[74] It is shown in Figures 6 and 7 with *E*-**36**.
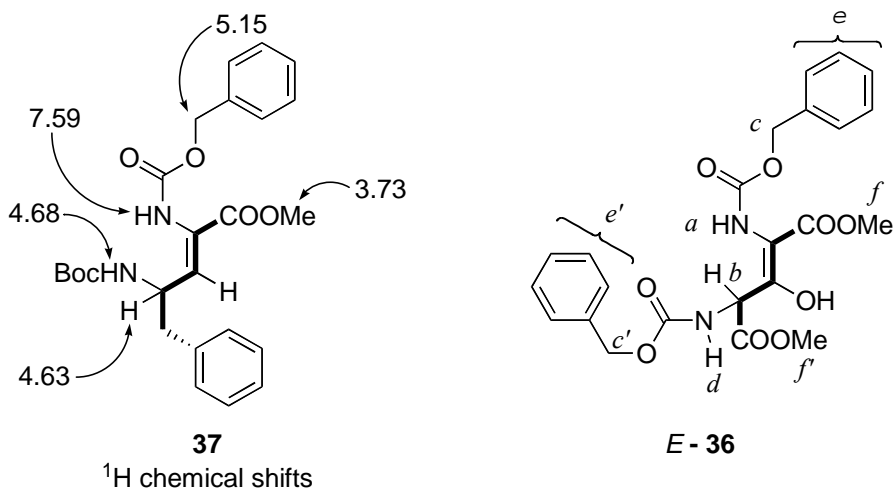
Figure 6. Model compound used to assign [^1]H NMR chemical shifts in **36**.

From Figure 6, we may predict the chemical shifts of the protons in compound **36**. The peaks can be reasonably assigned as follows (note: the peaks came out pairs indicate the two diastereoisomers, *E*-**36** and *Z*-**36**): 8.0 ppm (broad peaks), CbzN*H*C=C (H*a*); 5.8 ppm and 5.9 ppm, four peaks also indicate four kind of C=CC*H* (H*b*) as the methyl ester groups; 5.1 ppm, OC*H₂*Ph (H*c*/H*c'*); 4.8 ppm and 4.9 ppm (broad peaks), CbzN*H*CH (H*d*); 7.2~7.5 ppm (multiple peaks), phenyl protons (H*e*/H*e'*); 3.6~3.7 ppm methyl groups (H*f*/H*f'*).

We may also assign the [^13]C peaks of compound **36** regarding the model compound **37** (Figure 7) as follows: 54.5 and 54.7 ppm, 53.3 ppm and 53.2 ppm, methyl group (C*a* and C*a'*); other peaks around 53 ppm, HNC*H* (C*b*); 67.3~68.7 ppm, OC*H₂*Ph (C*c* and C*c'*); 128~129 ppm, aromatic carbon (C*d* and C*d'*); 134.5 ppm and 134.7 ppm, NH*C*=COH (C*e*); 136.2 ppm and 136.4 ppm, NHC=*C*OH (C*f*, due to the −OH, the

chemical shift is downfield); 151.6 ppm and 156.5 ppm, $COOCH_2Ph$ (Cg and Cg'); 167.6 ppm and 167.8 ppm, $CHCOOMe$ (Ch), 170.2 ppm and 170.5 ppm, $C=CCOOMe$ (Ci).
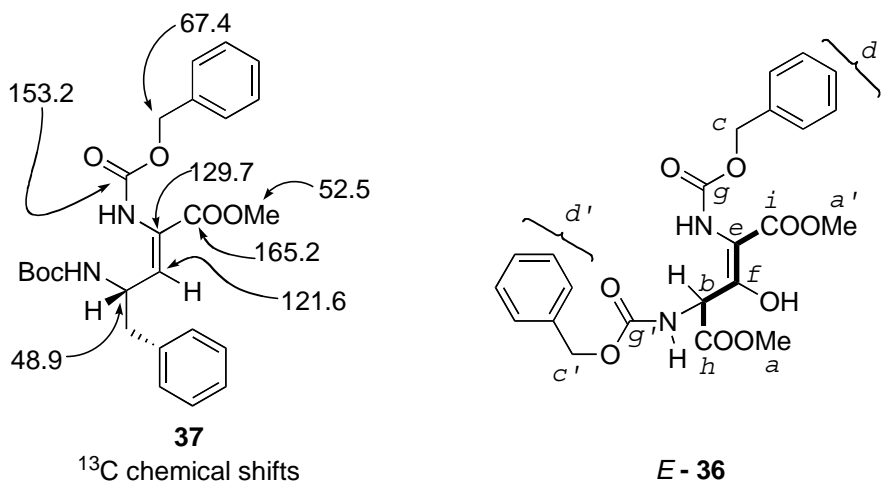
Figure 7. Model compound used to assign ^{13}C NMR chemical shifts in **36**.

2.3. N-H insertion of Rh(II)-stablilized carbenoid from bis(diazo) compound 33 into Boc-NH$_2$.

The *t*-butyl carbamate (Boc-NH$_2$) **40**, which was required for the N-H insertion reaction of dimethyl 2,4-bis(diazo)-3-oxoglutarate **33**, was easily afforded by bubbling dry ammonia gas through an ethanol solution of *t*-butyl dicarbonate **40** at 0 °C. (eq 18)
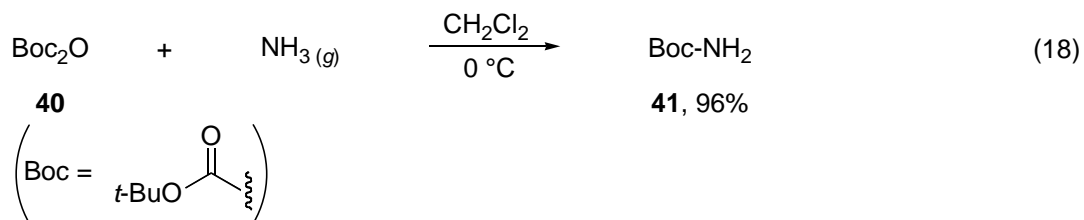
Dimethyl 2,4-bis(diazo)-3-oxoglutarate **33** reacted with excess *t*-butyl carbamate

41 in refluxing methylene chloride, catalyzed by $Rh_2(OAc)_4$. After the reaction solution

had refluxed for 1 h, the TLC showed bis(diazo) compound **33** was completely consumed.

Further purification by silica gel chromatography provided a colorless oil in 46% yield.

As discussed in section **2.2**, the N-H insertion reaction product **42** consists of two enol

forms *E*-**42** and *Z*-**42**. The NMR spectrum indicated the ratio of these two isomers was

E-**42**: *Z*-**42** = 67:33.

Scheme 15
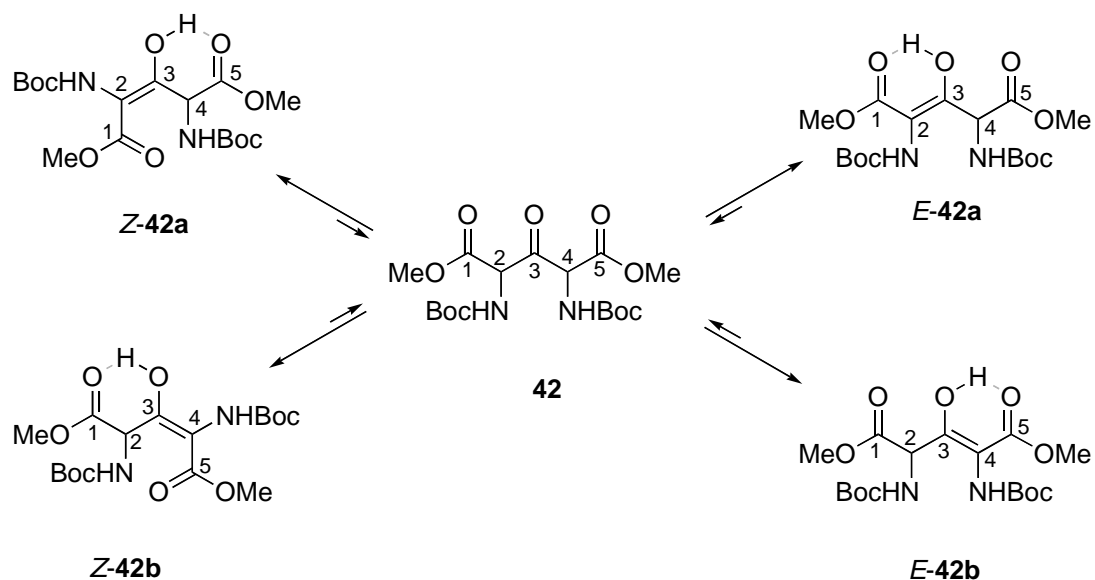
Finally, we were able to get bisprotected diamino dicarboxylic acids **36** and **42**.

Stereocontrol of the insertion products was impossible because of extensive enolization.

Nevertheless, the successful double N-H insertion reaction of the new bisdiazo

compound **33** reflects a further synthesis value on X-H (X = C, N, O, S, Se, P, halogen) insertion reactions.

2.4. Catalytic hydrogenolysis of N-H insertion reaction products.

Reduction of the ketone functionality of **36** and **42** to an alcohol (or CH_2) was the next goal. First we tried the reaction shown in eq. 19, hoping to reduce the central "ketone" while simultaneously deprotecting the amines by hydrogenolysis of the Cbz groups. We hoped that hydrogenation of these two enols **36** and **42** over Pd catalysts would achieve that goal. The reported hydrogenations of similar enolic substances caused us to be optimistic. (eq. 21).[54] The reaction was run in either methanol or 1,4-dioxane solvent.

$$(19)$$

$$(20)$$

$$R \underset{\text{O}}{\overset{\text{O} \quad \text{HO}}{\diagdown}} OR' \quad \xrightarrow[\text{modifier}]{\text{H}_2,\ \text{Pt/Al}_2\text{O}_3} \quad R \underset{\text{O}}{\overset{\text{O} \quad \text{OH}}{\diagdown}} OR' \qquad (21)$$
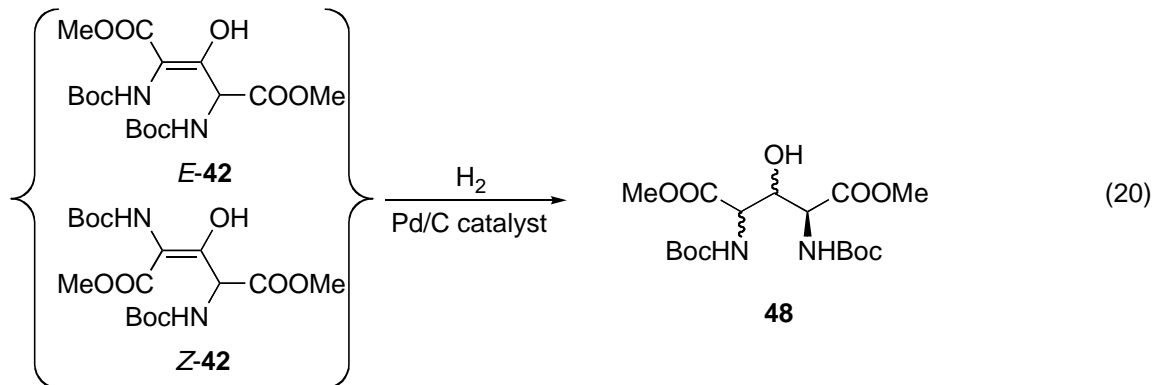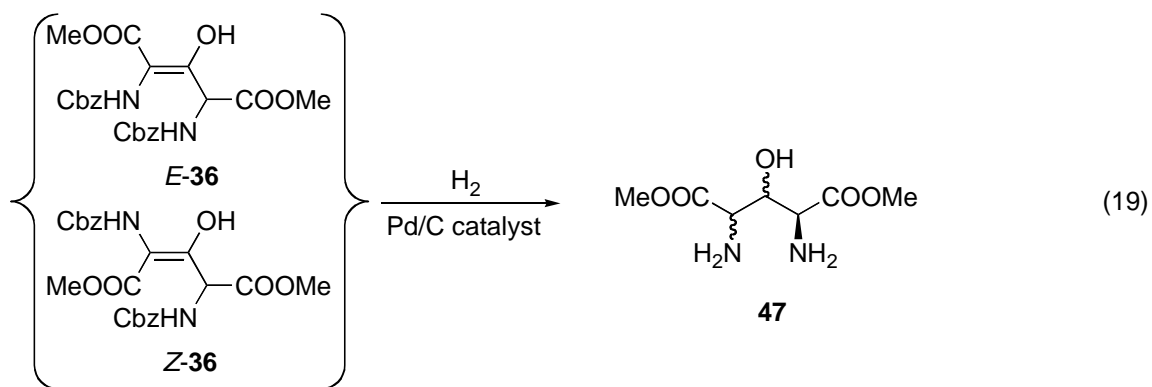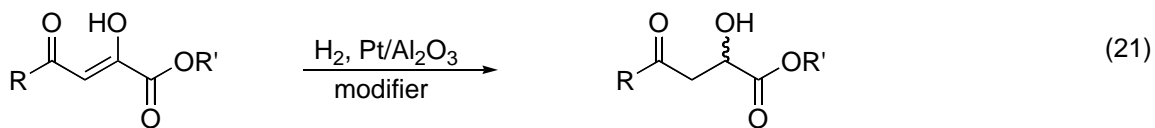
R = Me, t-Bu, Ph
R' = Et, H
modifier - HCd or HCn to improve the *ee*
HCd = 10,11-dihydrocinchonidine
HCn = 10,11-dihydrocinchonine

After hydrogenation under 40 psi H_2, compound **36** yielded white crystals after purification. However, the ^{1}H NMR spectrum gave an unexpected result. A doublet signal at 3.0 ppm coupled with triplet signal at 3.7 ppm indicated that there is a $-CH_2-CH-$ group in the structure which did not match any groups of compound **28**. Fortunately, we were able to obtain the x-ray structure of this strange product **44** (Figure 8). The crystal structure data are included in Appendix A.
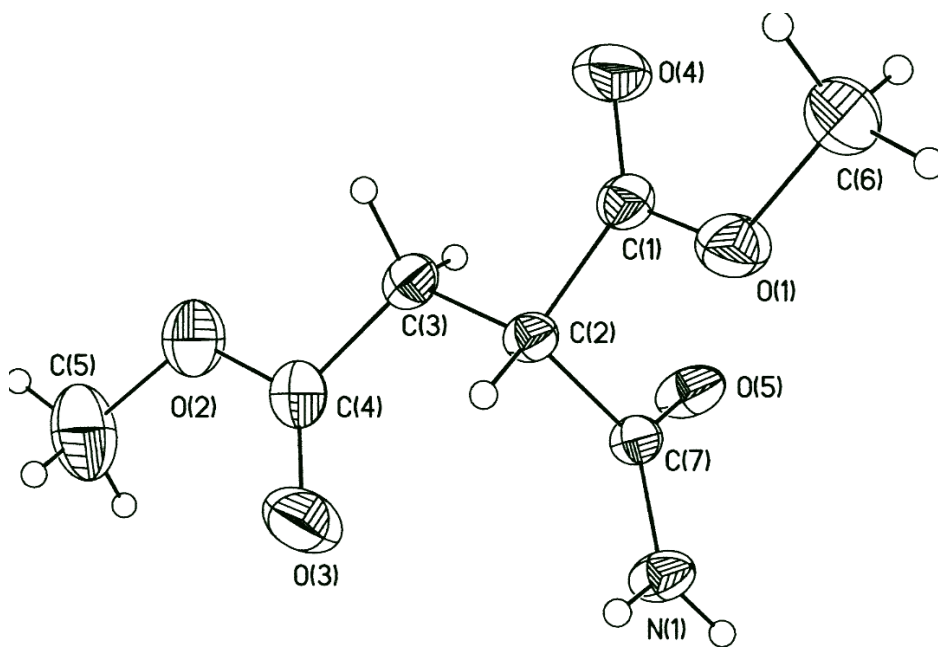
Figure 8. X-ray structure of compound **44**

A big question came to our mind. Why would we get compound **44**? We examined a sample of **36** by NMR after establishing the structure of **44** to check whether **36** had decomposed or rearranged on storage. It had not.

36

44
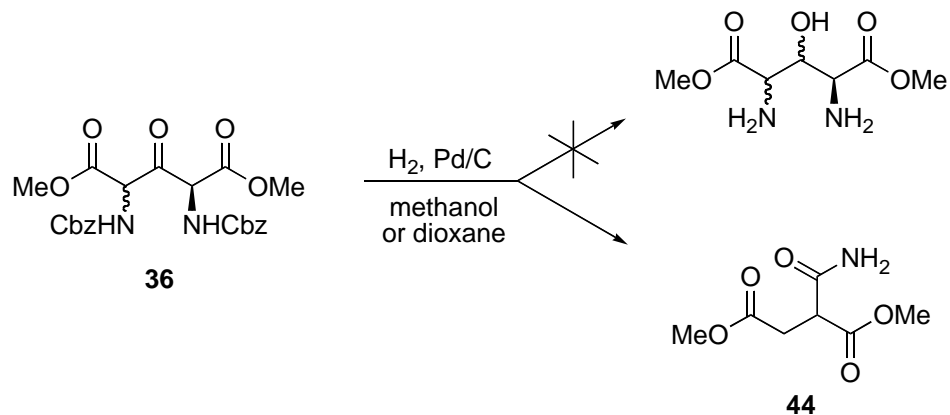
After searching the literature, we found a few examples which seemed to be related to the mechanism by which **44** is produced. Equation 22 illustrates the unusual formation of N-benzylamines during Cbz group hydrogenolysis.[67] Equation 23[75] is an example which illustrates the formation of a nucleophilic intermediate (in this case an enolate) during catalytic hydrogenation. These precedents support us to propose a mechanism for the hydrogenolysis of compound **36** on Pd/C catalyst (Scheme 18).

(22)

$$\text{(23)}$$

72%
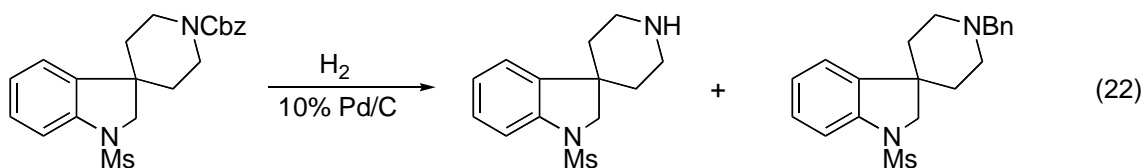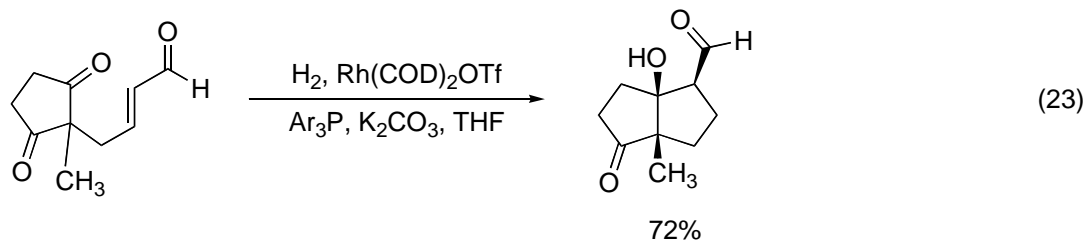
We postulate that in several steps **49** is formed by routine deprotection of the "righthand" NHCbz group (as drawn in Scheme 16) and deprotection followed by C-N hydrogenolysis of the "lefthand" NHCbz group. The next step is similar to eq. 23 in which a nucleophilic species attacks a neighboring carbonyl carbon. Cyclopropane **50** opens to relieve ring strain, giving **51** and hydroxide. Hydroxide adds to **51** in Michael fashion to give **52**, which loses hydride (perhaps to **49**), giving **53**. This tautomerizes to **44**. This mechanism is highly speculative.
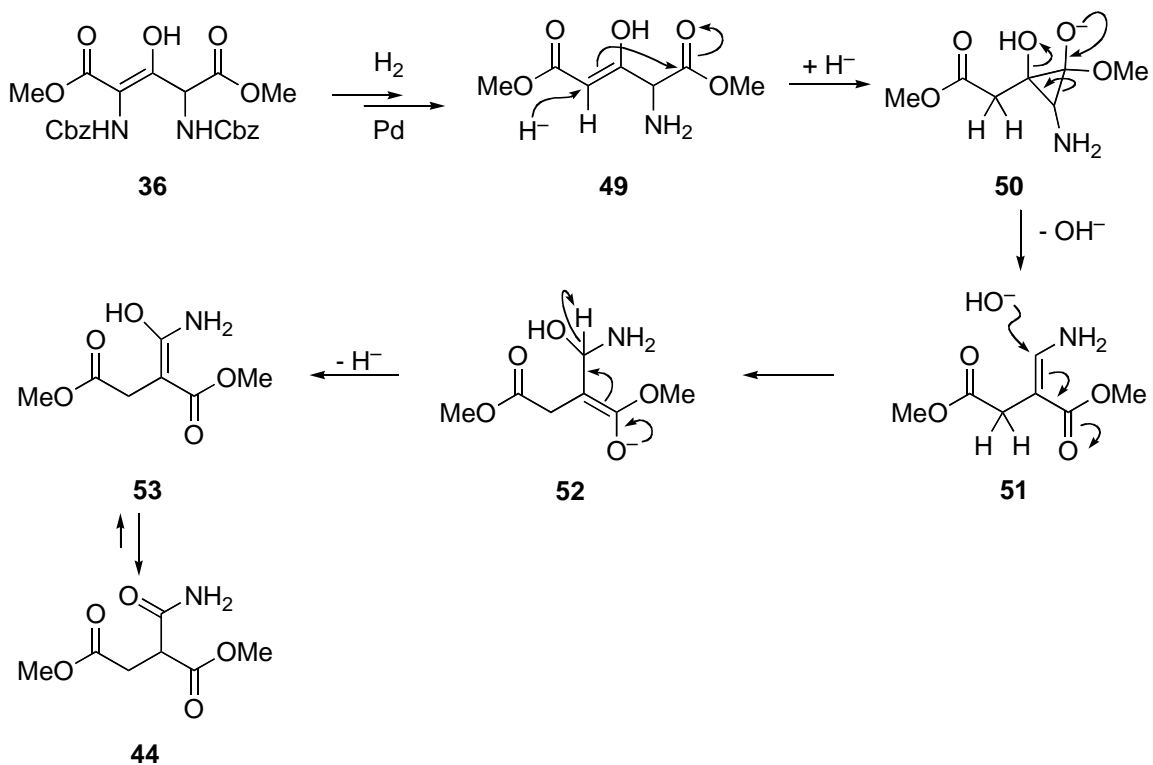
Scheme 16. Proposed mechanism for formation of **44**

We also tried Pd/C catalyzed hydrogenation of Boc-protected compound **42** which won't undergo the hydrogenolysis of Boc group. However, we only found the starting compound **42** instead of expected alcohol **48**.
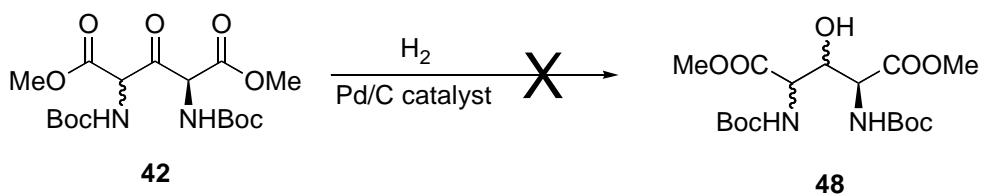
3. PART II. INTRODUCTION

3.1 Introduction to hypervalency.

The concept of hypervalent molecules was established by J. I. Musher in 1969.[55] Hypervalent compounds are ions or molecules of the elements bearing more electrons than the octet within a valence shell (Scheme 17). According to Musher,[55] there are essentially two ways to hold electrons beyond the octet within a valence shell: (1) make up a set of dsp^3 or d^2sp^3 hybrid orbitals using higher-lying d orbitals or (2) make up highly ionic orbitals revising the basic idea of Lewis that a covalent bond is formed by a localized pair of two electrons.
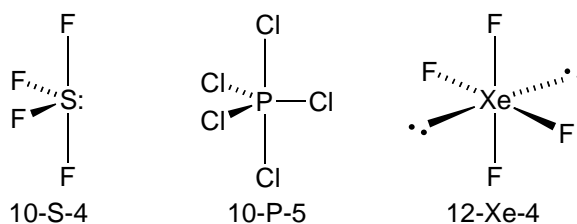
Scheme 17. Some simple hypervalent molecules

Pimentel and Rundle,[56] in 1951, laid the basis for new development in this area by proposing the idea of the three-center four-electron (3c-4e) bond, employing the molecular orbital theory. Owing to progress in computing and the efforts of many

43

scientists, the idea of the 3c-4e bond has become supported and is presently widely accepted.

The 3c-4e bond (Scheme 18) is an electron-rich, orbital-deficient bond and the nonbonding molecule orbital (NBMO) becomes HOMO while the antibonding orbital is the LUMO. Most hypervalent species will have a pseudo-trigonal bipyramidal geometry (TBP) that employs two types of bonding: hypervalent bonding to two apical ligands, and normal bonding to all equatorial ligands.[57]

Occupied   Occupied   Unoccupied
Bonding   Non-bonding   Antibonding
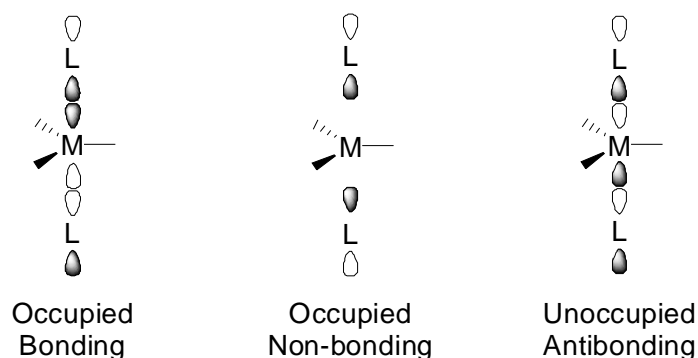
Scheme 18. Three-center four-electron (3c-4e), hypervalent bonding scheme

3.2 Hypervalent boron 10-B-5 species.

During the period when the interest in hypervalent species grew, very few hypervalent compounds of second-row elements were isolated or even detected. Only boron, carbon and fluorine species have been made so far, and there are only a small number of examples of these compounds. Some examples are the first hypervalent 10-B-5 boron compound **54** reported by Lee and Martin in 1984,[58] hypervalent 10-C-5

44

carbon compound **55** synthesized by Kin-Ya Akiba recently[59] (Scheme 19) and first

10-F-2 hypervalent fluorine species observed by Ault and Andrews in 1976,[60] which was

the highly unstable trifluoride anion F_3^- generated by simultaneous deposition of an

argon/fluorine mixture with CsF, RbF or KF and detected at low temperature by Raman

and infrared spectroscopy.
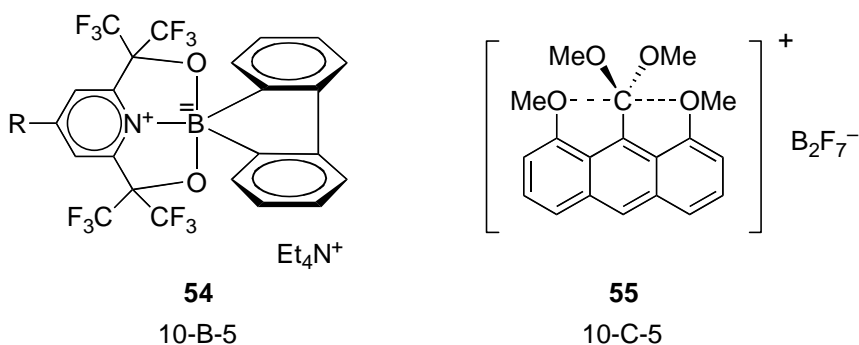
Scheme 19. Some hypervalent compounds based on second row elements.

Recently, Wada et al.[61] reported a synthesis route to tris(2,6-dimethoxyphenyl)-

borane **56** which let us set a program leading to a new 10-B-5 species **59** (Scheme 20). In

this thesis, we report on progress toward this goal.
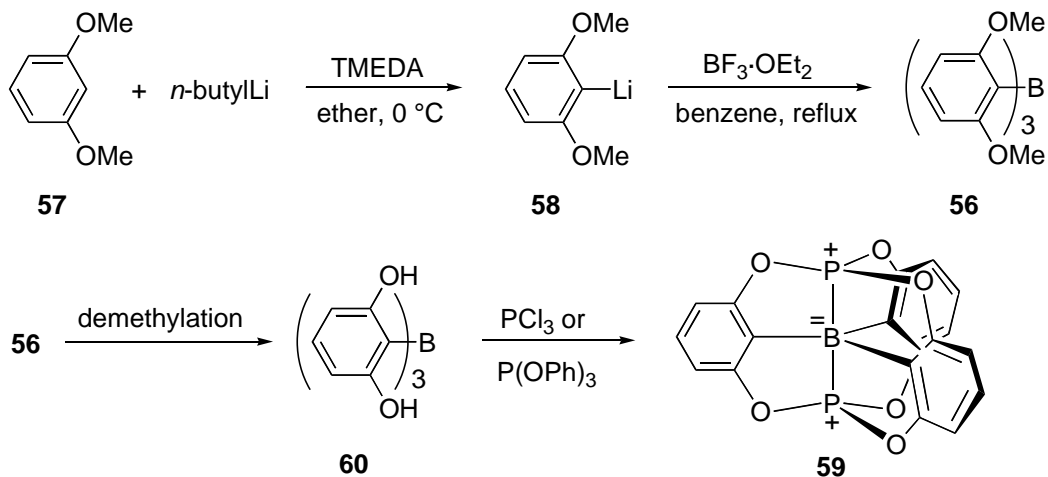
Scheme 20

3.3 Hypervalent phosphorus 10-P-5 species.

Phosphorus species **61** also attracted our interest (Scheme 23). It is formally an 8-P-5 species that may exhibit a three-center two-electron (3c-2e) bond. An analogous compound, **65,** was described recently.[72] Compound **65** was found to be undergoing a

65a
3c-2e bond

65b   **65c**
equilibrating 8-N-4 species
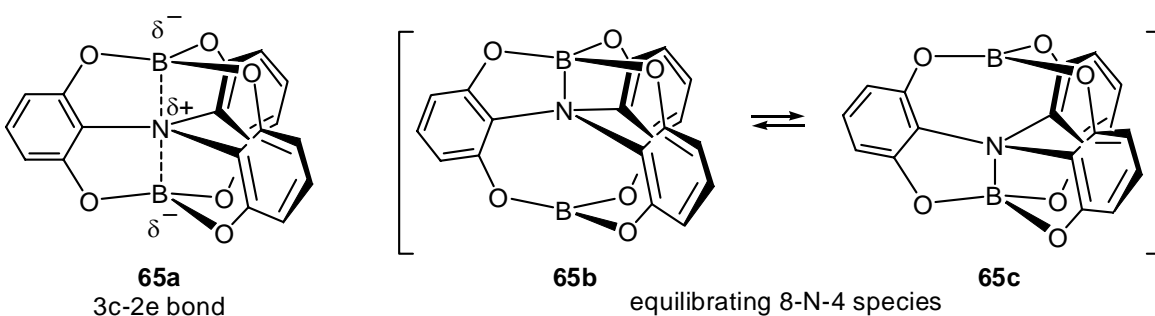
dynamic equilibrium in solution. The x-ray crystal structure of **65** revealed an unsymmetrical B-N-B triad (*i.e.* 6**5b** or **65c**), with the "free" boron coordinated to a

solvent THF molecule. It was of interest to see whether **61**, the phosphorus analogue of

65, would have a greater tendency than **65** to engage in three-center bonding.

Hui Li of our laboratory has made progress in the synthesis of **61**.[73] We report

herein our work directed at the completion of this synthesis.
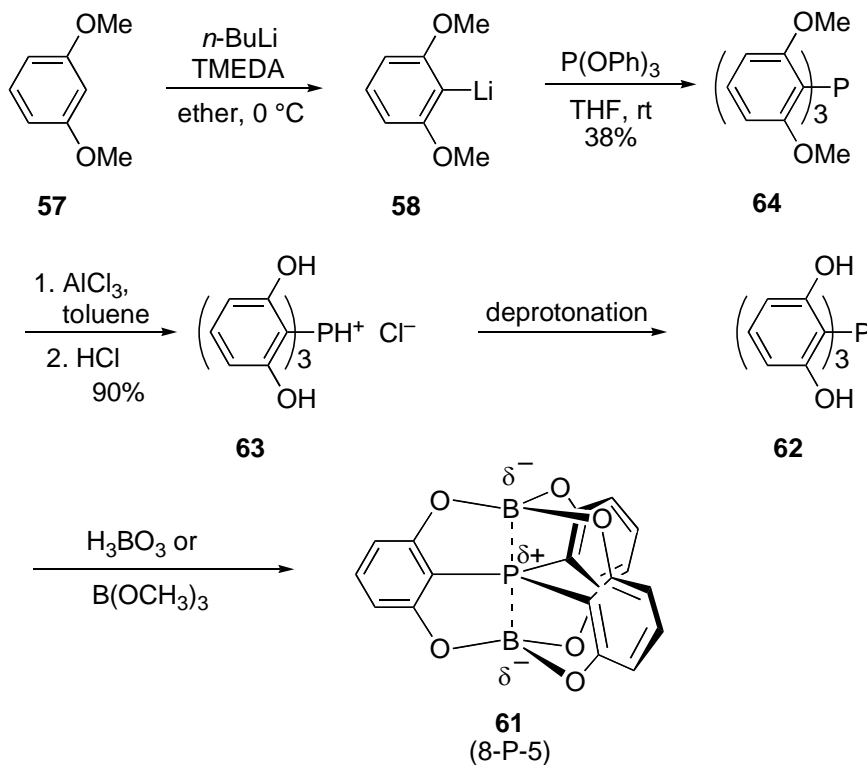
Scheme 21

4. PART II. RESULTS AND DISCUSSION

4.1 Synthesis of tris(2,6-dimethoxyphenyl)borane

Compound **56**, Φ_3B (the 2,6-dimethoxyphenyl group is sometimes denoted as "Φ"), was prepared by the reaction of ΦLi **58** and boron trifluoride diethyl etherate.[61] To a solution of 1,3-dimethoxybenzene **57** and a catalytic amount of *N,N,N',N'*-tetramethyl-ethylenediamine (TMEDA) in diethyl ether was added a 2.5 M *n*-hexane solution of *n*-butyllithium at 0 °C under nitrogen. To the suspension of ΦLi **58** after precipitates formed was added boron trifluoride diethyl etherate in benzene. After reflux and recrystallization from THF, white crystals of Φ_3B **56** were obtained in 41% yield for both steps (eq. 24).
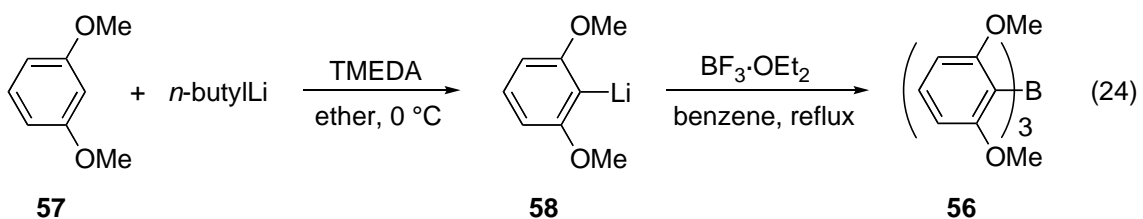
4.2 Demethylation of tris(2,6-dimethoxyphenyl)borane, 56.

Many reagents have been utilized for demethylation of aryl methyl ethers as reported in the chemical literature. The most commonly used are hydrogen iodide (or

bromide),[62] boron tribromide,[63] trimethylsilyl iodide,[64] aluminum chloride,[65] pyridinium hydrochloride,[65] and sodium amide.[66] In our research here, we have tried aluminum trichloride and boron tribromide so far.

4.2.1 Demethylation of 56 by aluminum trichloride.

To the fine suspension of Φ_3B **56** in toluene was added anhydrous AlCl$_3$ under nitrogen. After reflux, water was added to hydrolyze the excess AlCl$_3$. However, the white solid obtained proved to be resorcinol **66** by NMR spectrum (eq. 25). The unexpected decomposition indicates that the carbon-boron bonds in **56** were cleaved, although the demethylation still occurred.
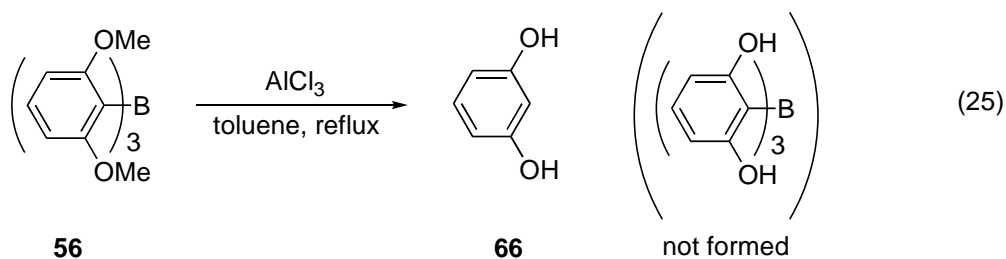
4.2.2 Demethylation by BBr$_3$·S(Me)$_2$.

BBr$_3$ is another commonly used demethylation reagent which came to mind after AlCl$_3$ failed to afford desired tris(2,6-dihydroxyphenyl)borane. To the solution of Φ_3B **56** in methylene chloride was added a solution of BBr$_3$·S(Me)$_2$ complex in methylene chloride at 0 °C under nitrogen. The afforded mixture indicated that the demethylation only partially occurred and we still detect resorcinol in the product by NMR spectrum (eq. 26).

$$\underset{\textbf{56}}{\left(\begin{array}{c} OMe \\ \\ B \\ \\ OMe \end{array}\right)_3} \xrightarrow[\text{CH}_2\text{Cl}_2,\ \text{rt}]{\text{BBr}_3\cdot\text{S(Me)}_2} \underset{\textbf{66}}{\begin{array}{c} OH \\ \\ OH \end{array}} + \text{partial demethylation products} \qquad (26)$$
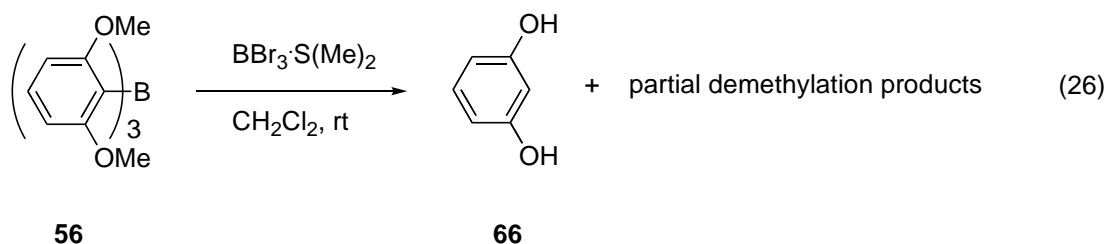
The demethylation of **56** to target product could not be accomplished by either AlCl₃ or BBr₃. Because of the time limit, further investigation of the demethylation of **56** has not been done yet. When choosing other demethylation reagents, the cleavage of the carbon-boron bond of $\varPhi_3$B **56** might be avoided by avoiding acidic conditions, which seem to promote C-B cleavage.

4.3 Synthesis of tris(2,6-dihydroxyphenyl)phosphonium chloride 63.

The synthesis of compound **63** has been well developed by Hui Li in his previous work in our laboratory[73] as shown in Scheme 21. Tris(2,6-dimethoxyphenyl)phosphine **64** can be prepared by adding the triphenyl phosphite to **58** which was the product of ortho-lithiation of 1,3-dimethoxybenzene **57** in THF. Further demethylation of tris(2,6-dimethoxyphenyl)phosphine **64** by anhydrous AlCl₃ in toluene afforded a red solid.
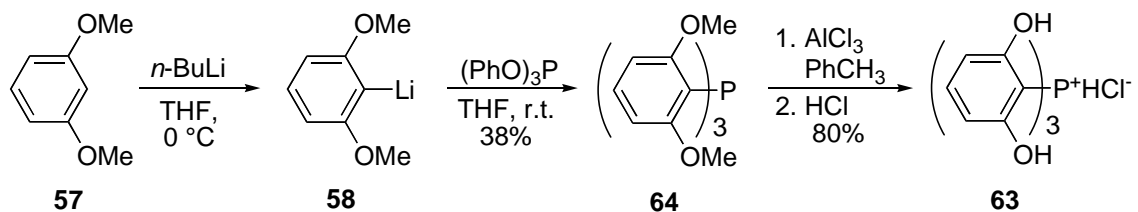
Scheme 22

By recrystallization from EtOEt/MeOH, a single crystal suitable for x-ray diffraction was obtained. The crystal was found to be a co-crystal with the ethyl ether, which was revealed by proton NMR. This indicated the hydrogen bond between compound **63** and solvent is strong which also was found that compound **63** associated with ethyl acetate from Hui Li's research.[73] A structure diagram is provided in Figure 9 and crystal structure data are included in Appendix B. We are interested in the bond lengths and bond angles of phosphorus to the neighboring atoms which are indicated in Table 1.
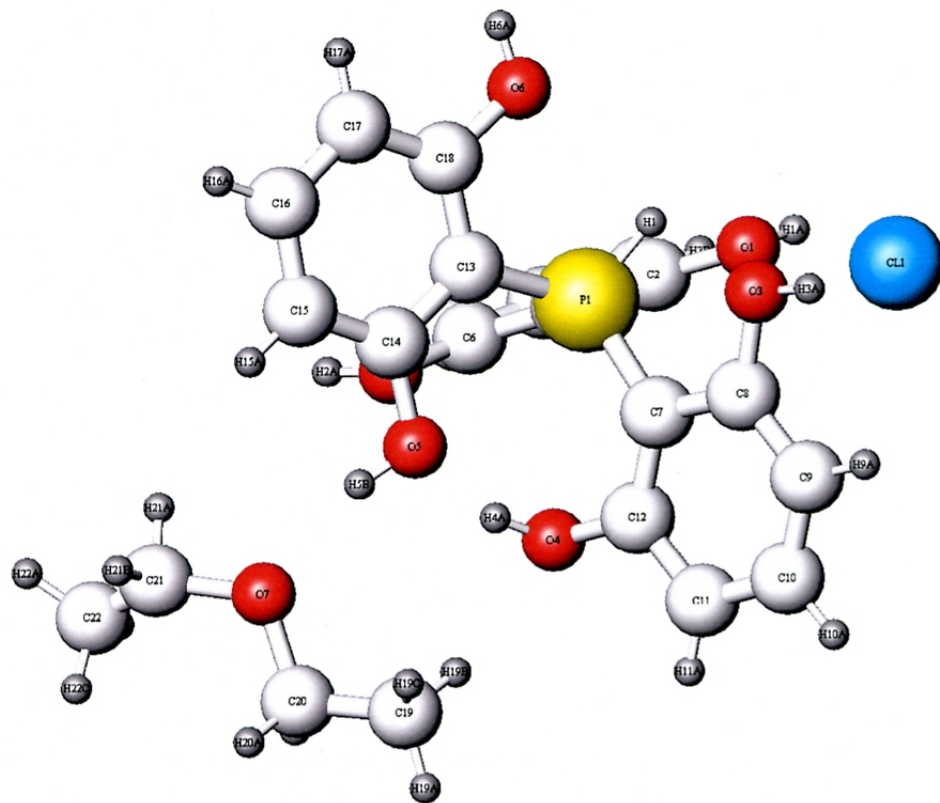
Figure 9. Crystal structure of compound **63**

Parameters	Bond length (Å)	Bond angle (°)	Torsion angle (°)
P(1)-C(13)	1.770(3)		
P(1)-C(7)	1.770(3)		
P(1)-C(1)	1.786(2)		
P(1)-H(1)	1.27(2)		
C(13)-P(1)-C(7)		114.84(12)	
C(13)-P(1)-C(1)		113.68(12)	
C(7)-P(1)-C(1)		112.37(12)	
H(1)-P(1)-C(1)		104.7(11)	
H(1)-P(1)-C(7)		104.0(10)	
H(1)-P(1)-C(13)		106.0(11)	
H(1)-P(1)-C(1)-C(2)			30.8(11)
H(1)-P(1)-C(7)-C(8)			20.5(11)
H(1)-P(1)-C(13)-C(14)			24.5(11)

Table 1. Selected Structural Parameters of **63**
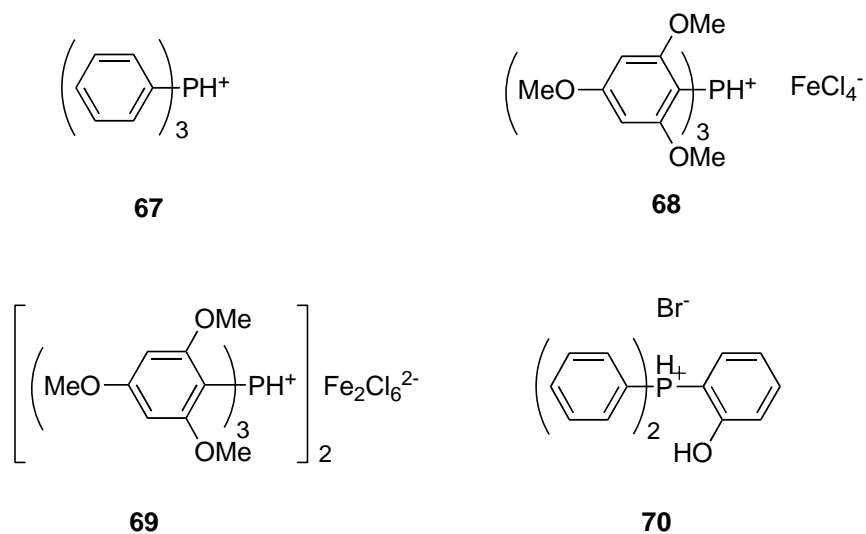
Scheme 23

The P(1), C(1), C(7) and C(13) formed an asymmetric pyramid with the equal length of P(1)-C(7) and P(1)-C(13). A search of the crystallographic literature revealed several reports of structures of the type $(Ar_3PH)^+$. The majority of crystal structures which were found involved the triphenylphosphonium ion, Ph_3PH^+, **67**.[70] Other more relevant examples were: tris(2,4,6-trimethoxyphenyl)phosphonium tetrachloroiron(III) **68**[68], bis{tris(2,4,6-trimethoxylphenyl)phosphonium} bis[(μ_2-chloro)-dichloroiron] **69**[69], (2-hydroxyphenyl)diphenylphosphonium bromide **70**[71] (Scheme 25). Geometrical parameters of these phosphonium ions are compared to those of **63** in Table 2.

Parameters	63	67[a]	68	69	70
h (Å)	-	0.525(16)	0.481	0.541	0.542
average P-C bond length (Å)	1.771(8)	1.786(8)	1.783(6)	1.791(7)	1.786(2)
P-H bond length(Å)	1.27(2)	1.351(6)	1.438	1.612	1.413
average C-P-C bond angle (°)	113.6(2)	110.7(5)	113.0(3)	111.3(2)	111.2(2)
average C-P-H bond angle (°)	104.9(4)	108.2(14)	105.7(4)	107.7(6)	107.4(7)

[a] values are averages of all reported triphenylphosphonium ion structures

Table 2.

We first thought that the parameters of compound **63** would be similar to those of compound **70** because compound **70** has –OH on its phenyl ring. However, from the Table above, the P-C bond length, C-P-C bond angle and C-P-H bond angle of compound **63** are most close to compound **68**. The P-H bond length of compound **63** is much less than either the average P-H bond length of triphenylphosphonium ion or the other triarylphosphonium ions.

We have been able to synthesis tris(2,6-dihydroxyphenyl)phosphonium chloride **63** and determine its structure. The next step is to deprotonate **63** by base (Scheme 21) which is a key step in the synthesis of compound **61** and the study of multicenter, perhaps hypervalent, bonding between the phosphorus and boron or other main group elements.

5. EXPERIMENTAL

General: Methylene chloride and acetonitrile were distilled over calcium hydride under nitrogen atmosphere. Reagents used in the syntheses were purchased from the Aldrich Chemical Company and were used without further treatment.

Melting points were recorded on a capillary melting point apparatus and are uncorrected. NMR spectra were obtained at room temperature from Bruker AV-400 spectrometer operating at 400 MHz for ^{1}H and 100 MHz for ^{13}C. TMS was used as internal standard. The results are presented as parts per million (ppm or δ) and coupling constants are reported in Hz.

Mass spectral (MS) data were obtained using either a Finnegan 3300 or a VG 7070E mass spectrometer using a solid probe. The results are presented in terms of intensity percentage relative to the base peak and probable fragmentation product.

Elemental analysis was performed by Atlantic Microanalytical lab, GA.

TLC was performed on Sorbent Technologies silica G TLC plates w/UV254. Preparative column chromatography employed Sorbent Technologies silica gel (60 Å, 32-63 μm).

***p*-Acetoamidobenzenesulfonyl azide, 7.**[52] To a suspension of *p*-acetamido-benzenesulfonyl chloride **13** (50.0 g, 0.214 mol) in 400 ml methylene chloride containing

tetrabutylammonium bromide (0.200 g, 0.008 mmol) at 0 °C was added dropwise a solution of sodium azide (16.0 g, 0.248 mol, in 50 mL H_2O). The reaction was allowed to warm up to rt and was kept stirring at rt for 16 h. The organic layer was separated and washed with water (2 x 75 mL) and saturated aqueous sodium chloride (2 x 50 mL), dried over Na_2SO_4 and evaporated to give 46.9 g (91.3%) pure white solid, mp 107-110 °C. ^{1}H NMR (400 MHz, $CDCl_3$): 2.25 (s, 3H), 7.80 (m, 2H), 7.89 (m, 2H), 8.04(br, 1H). ^{13}C NMR (100 MHz, $CDCl_3$): 25.0, 119.8, 129.2, 132.7, 144.2, 169.3.

Dimethyl 2,4-bis(diazo)-3-oxoglutarate, 33. To a stirred solution of dimethyl 3-oxoglutarate **34** (2.41 g, 13.9 mmol) and triethylamine (3.00 g, 29.7 mmol) in 45 mL acetonitrile at 0 °C was added dropwise *p*-acetamidobenzenesulfonyl azide 7 (7.20 g, 30.0 mmol) in 100 mL acetonitrile over 30 minutes. The reaction was allowed to warm to rt and stirred for 12 h. The reaction mixture was filtered and the filtrate was evaporated under reduced pressure. The residue was washed with ethyl acetate/hexanes (1:1), filtered, and the solvent was evaporated. Further purification by silica gel column chromatography (hexanes/ethyl acetate = 4:1) gave 2.86 g yellow oil (92%). ^{1}H NMR (400 MHz, $CDCl_3$): 3.83 (s). ^{13}C NMR (100 MHz, $CDCl_3$): 52.8, 74.2, 161.4, 174.5. IR (neat): 3004.6, 2956.0, 2133.3, 1719.0, 1601.2, 1433.9, 1321.4, 1192.3, 1126.2, 996.1, 750.1, 763.1, 698.9. Anal. Calcd. for $C_7H_6O_5N_4$: C, 37.18; H, 2.67; N, 24.77. Found: C, 37.15; H, 2.69; N, 24.53.

Benzyl carbamate, 35. To a stirred solution of benzyl chloroformate (10.3 g,

0.063 mol) in 200 mL methylene chloride was bubbled through dry ammonia gas at 0 °C. Stopped bubbling while there was no more precipitation formed. Filtered the precipitation and the filtrate was evaporated under reduced pressure to give 9.10 g (99%) white crystals, mp 87-88 °C. ^{1}H NMR (400 MHz, CDCl$_3$): 4.89 (br, 2H), 5.10 (s, 2H), 7.36 (m, 5H). ^{13}C NMR (100 MHz, CDCl$_3$): 67.1, 128.3, 128.4, 128.8, 136.4, 157.0.

Compound 36. To a stirred solution of dimethyl 2,4-bis(diazo)-3-oxoglutarate **33** (0.300 g, 1.33 mmol) in 15 mL methylene chloride was mixed with benzyl carbamate **35** (0.401 g, 2.66 mmol). A catalytic amount of rhodium(II) acetate (24 mg, 0.05 mmol) was added. The reaction set up was then immediately moved to a pre-heated oil bath at 42℃. After refluxing for 3 h, the bis(diazo) compound was completely consumed. The reaction mixture was purified by silica gel column chromatography (first using hexanes/ethyl acetate = 1:1 washing out the fractions before yellow band. The afforded fractions were separated by hexanes/ethyl acetate = 5:1) gave 0.430 g (68%) colorless oil. ^{1}H NMR (400 MHz, CDCl$_3$): 3.67 (s, 3H), 3.71 (s, 3H), 4.96 (br, d, J = 3.2 Hz, 1H), 5.98 (d, J = 10.3Hz, 1H), 7.95 (br, 1H) for one isomer; 3.73 (s, 3H), 3.75 (s, 3H), 4.79 (br, 1H), 5.82 (d, J = 9.2 Hz, 1H), 8.17 (br, d, J = 1.2 Hz, 1H) for the other isomer, 5.15 (m, 5H, two CH_2Ph, OH), 7.33 (m, 10H). ^{13}C NMR (100 MHz, CDCl$_3$): 52. 8, 53.2, 53.2, 53.3, 53.3, 53.4, 128.1, 128.3, 128.3, 128.4, 128.7, 128.7, 128.7, 128.8, 128.92, 128.94, 129.03, 129.03, 134.6, 134.7, 136.2, 136.4, 151.6, 156.2, 156.5, 167.6, 167.9, 170.2, 170.5.

***t*-Butyl carbamate, 41.** To a 50 mL saturated NH$_3$-EtOH solution was added

dropwise a solution of t-butyl dicarbonate **40** (21.3 g, 97.8 mmol) in 50 mL ethanol at 0 °C. While stirring, the solution was bubbled through dry ammonia gas. Stopped bubbling while there was no more precipitation formed. Filtered the precipitation and the filtrate was evaporated under reduced pressure. Added 50 mL hexane. Boiled at 65 °C for 30 minutes. Cooled down to 0 °C. Washed with hexane and dried to give 11.0 g (96%) white crystals, mp 106-108 °C. ^{1}H NMR (400 MHz, CDCl$_3$): 1.45 (s, 9H), 4.67 (br, 2H). ^{13}C NMR (100 MHz, CDCl$_3$): 28.4, 79.8, 156.7.

Compound 42. To a stirred solution of dimethyl 2,4-bis(diazo)-3-oxoglutarate **33** (1.94 g, 8.58 mmol) in 100 mL methylene chloride was mixed with *t*-butyl carbamate **41** (2.10 g, 17.9 mmol). A catalytic amount of rhodium(II)acetate (40 mg, 0.1 mmol) was added. The reaction set-up was then immediately moved to pre-heated oil bath at 42℃. After refluxing for 3 h, the bisdiazo compound was completely consumed. The reaction mixture was purified by silica gel column chromatography (first using hexanes/ethyl acetate = 1:1 washing out the fractions before yellow band. The afforded fractions were separated by hexanes/ethyl acetate = 5:1) gave 1.59 g (46%) colorless oil. ^{1}H NMR (400 MHz, CDCl$_3$): 1.44 (s, 9H), 1.48 (s, 9H), 3.74 (s, 3H), 3.75 (s, 3H), 4.90 (br, 1H), 5.06 (dd, J_A = 10.4Hz, J_B = 4.00Hz, 1H), 5.71 (d, J = 10.4Hz, 1H), 7.68 (br, 1H) for one isomer; 1.45 (s, 9H), 1.49 (s, 9H), 3.74 (s, 3H), 3.78 (s, 3H), 4.69 (br, 1H), 5.14 (dd, J_A = 9.1 Hz, J_B = 3.6 Hz, 1H), 5.55 (d, J = 9.2 Hz, 1H), 7.96 (br, 1H) for the other isomer. ^{13}C NMR (100 MHz, CDCl$_3$): 28.1, 28.1, 28.4, 28.4, 52.8, 53.0, 53.1, 53.2, 54.7, 54.8, 62.3,

63.4, 80.3, 80.6, 83.6, 83.8, 128.4, 129.2, 150.0, 150.4, 155.6, 155.8, 168.0, 168.4, 170.8, 170.9.

Tris(2,6-dimethoxyphenyl)borane, 56.[61] To a solution of 1,3-dimethoxybenzene **57** (5.52 g, 40.0 mmol) and a catalytic amount of *N,N,N',N'*-tetramethylethylenediamine (TMEDA, 0.2 mL) in diethyl ether (50 mL) was added a 2.5 M n-hexane solution of *n*-butyllithium (16 mL, 40 mmol) at 0 °C under nitrogen. The mixture was stirred for 3 h to afford the precipitate of ΦLi **58**. To this suspension was added boron trifluoride diethyl etherate (1.89 g, 13.2 mmol) in benzene (50 mL) and the mixture was refluxed for 4 h. 15 mL methanol was added at rt and the insoluble materials were recrystallized from THF to give 2.27 g (41%) white crystals of Φ_3B **56**. m.p.: 234-235 °C. ^{1}H NMR (400 MHz, CDCl$_3$): 3.45 (s, 18H), 6.47 (d, J = 8.2 Hz, 6H), 7.18 (t, J = 8.2 Hz, 3H). ^{13}C NMR (100 MHz, CDCl$_3$): 56.8, 105.3, 130.3, 162.7.

Tris(2,6-dimethoxyphenyl)phosphine, 64. To a solution of 1,3-dimethoxy-benzene **57** (10.0 g, 72.5 mmol) in THF (40 mL) was added a 2.5 M *n*-hexane solution of *n*-butyllithium (30.5 mL, 76.3 mmol) at 0 °C under nitrogen. After stirring at 0 °C for 45 minutes, a solution of triphenyl phosphite (6.75 g, 21.8 mmol) in THF (20 mL) was added dropwise. Then the stirring was continued overnight at rt. The reaction was quenched by adding a few mL methanol. Filtered the solid, washed with ether, combined the filtrate and the ether. Evaporate the solvent and wash the solid by water. The solid was recrystallized from acetone/water to give 3.61 g (37.5%) white crystals. m.p.:

149-151 °C. ^{1}H NMR (400 MHz, CDCl$_3$): 3.48 (s, 18H), 6.44 (dd, J_A = 8.2 Hz, J_B = 2.9

Hz, 6H), 7.13 (t, J = 8.0 Hz, 3H). ^{13}C NMR (100 MHz, CDCl$_3$): 56.2, 104.5, 115.5, 128.7,

162.5, 162.6. ^{31}P NMR (162 MHz, CDCl$_3$): -66.6.

Tris(2,6-dihydroxyphenyl)phosphonium chloride 63. Anhydrous AlCl$_3$ (810

mg, 6.07 mmol) was added to a fine suspension of tris(2,6-dimethoxyphenyl)phosphine

64 (442 mg, 1.00 mmol) in 15 mL dry toluene under nitrogen. The suspension was

refluxed for 2 h and the stirred at rt overnight, which resulted in much gray-green

precipitate. The reaction was quenched by slow addition of 15 mL 3 M HCl and the

insoluble material changed color to pink. The stirring was continued until none of the

precipitate stuck to the glass. The solid was collected by filtration and washed with

diethyl ether, and dried on the vacuum line, which afforded 308 mg (80%) almost pure

compound **63**. Further purification can be achieved by recrystallization from Et$_2$O/MeOH,

mp 234 °C. ^{1}H NMR (400 MHz, DMSO-d_6): 6.36 (dd, J = 5.6 Hz, 7.6 Hz, 6H), 7.22 (t,

J = 8.1 Hz, 3H), 8.37 (d, J = 534 Hz, 1H), 10.63 (s, 6H). ^{13}C NMR (100 MHz, DMSO-d_6):

93.2 (d, J = 102 Hz), 107.0 (d, J = 5.7 Hz), 136.3, 162.3. ^{31}P NMR (162 MHz, DMSO-d_6):

-51.3 (d, J = 527 Hz).

6. REFERENCES

1. Curtius,, T. *Chem. Ber.* **1883**, *16*, 2230-2231.

2. Curtius, T. *J. Prakt. Chem.* **1888**, *38*, 396-440.

3. Arndt, F.; Eistert, B.; Partale, W. *Chem. Ber.* **1927**, *60B*, 1364-1370.

4. Arndt, F.; Amende, J. *Chem. Ber.* **1928**, *61B*, 1122-1124.

5. Arndt, F.; Eistert, B.; Amende, J. *Chem. Ber.* **1928**, *61B*, 1949-1953.

6. Bradley, W.; Robinson, R. *J. Chem. Soc.* **1928**, 1310-1318.

7. Doyle, M. P.; McKervey M. A.; Ye, Tao, "Catalysts for Metal Carbene Transformations," in *Modern Catalytic Methods for Organic Synthesis with Diazo Compounds*; Wiley, New York, 1998; Chapter 2.

8. Regitz, M., "Transfer of Diazo Groups," in *Newer Methods of Preparative Organic Chemistry; Vol. 6.* Foerst, W., Ed.; Academic Press: New York, **1971**, 81-126.

9. Saarbrücken, M. R. *Angew. Chem. Int. Ed. Engl.* **1966**, *5*, 681-682.

10. Doering, W von E.; DePuy, C. H. *J. Am. Chem. Soc.* **1953**, *75*, 5955-5957.

11. Hazen, G. G.; Weinstock, L. M.; Connell, R.; Bollinger, F. W. *Synth. Commun.* **1981**, *11(12)*, 947-956.

12. Bollinger, F. W.; Tuma, L. D. *Synlett.* **1996**, 407-413.

13. Doyle, M. P., "Catalytic Methods for Metal Carbene Transformations," *Chem. Rev.*

1986, *86*, 919-939.

14. McGarrity, J. F.; Smyth, T. *J. Am. Chem. Soc.* **1980**, *102*, 7303-7308.

15. McGarrity, J. F., "Basicity, Acidity and Hydrogen Bonding," in *The Chemistry of Diazonium and Diazo Groups*; Patai, S., Ed.; Wiley, New York, 1978; Part 1, Chapter 6.

16. Padwa, A.; Krumpe, K. E. *Tetrahedron* **1992**, *48*, 5385-5453.

17. Doyle, M. P. "Metal Carbene Complexes in Organic Synthesis: Diazo Decomposition-Insertion and Ylide Chemistry," in *Comprehensive Organometallic Chemistry II*; Hegedus, L. S., Ed.; Pergamon Press, New York, **1995**; Vol. 12, Chapter 5.2.

18. Davies, H. M. L. *Tetrahedron* **1993**, *49*, 5203-5223.

19. Padwa, A.; Austin, D. J. *Angew. Chem., Int. Ed. Engl.* **1994**, *33*, 1797-1815.

20. Maas, G., *Top. Curr. Chem.* **1987**, *137*, 76-253.

21. Kennedy, M.; McKervey, M. A.; Maguire, A. R.; Roos, G. H. P. *J. Chem. Soc., Chem. Commun.* **1990**, 361-362.

22. Doyle, M. P.; Winchester, W. R.; Hoorn, J. A. A.; Lynch, V.; Simonsen, S. H.; Ghosh, R. *J. Am. Chem. Soc.* **1993**, *115*, 9968-9978.

23. (a) Paulissen, R.; Reimlinger, H.; Hayez, E.; Hubert, A. J.; and Teyssié, P. *Tetrahedron Lett.* **1973**, 2233-2236. (b) Paulissen, R.; Hubert, A. J.; Teyssié, P. *Tetrahedron Lett.* **1974**, 607-608.

24. Moser, W. R. *J. Am. Chem. Soc.* **1969**, *91*, 1135-1140.

25. Cama, L. D.; Christensen, B. G. *Tetrahedron Lett.* **1978**, *19*, 4233-4236.

26. Salzmann, T. N.; Ratcliffe, R. W.; Christensen, B. H.; Bouffard, F. A. *J. Am. Chem. Soc.* **1980**, *102*, 6161-6163.

27. Melillo, D. G.; Shinkai, I.; Liu, T.; Ryan, K.; Sletzinger, M. *Tetrahedron Lett.* **1980**, *21*, 2783-2786.

28. Paulissen, R.; Hayez, E.; Hubert, A. J.; Teyssié, P. *Tetrahedron Lett.* **1974**, 607-608.

29. Landais, Y.; Planchenault, D. *Synlett* **1995**, 1191-93.

30. Bagley, M. C.; Buck, R. T.; Hind, S. L.; Moody, C. J.; Slawin, A. M. Z. *Synlett* **1996**, 825-826.

31. Osipov, S. N.; Sewald, N.; Kolomiets, A. F.; Fokin, A. V.; Burger, K. *Tetrahedron Lett.* **1996**, *37*, 615-618.

32. Moyer, M. P.; Feldman, P. L.; Rapoport, H. *J. Org. Chem.* **1985**, *50*, 5223-5230.

33. Doyle, M. P.; McKervey M. A.; Ye, T., "Catalysts for Metal Carbene Transformations," in *Modern Catalytic Methods for Organic Synthesis with Diazo Compounds*; Wiley, New York, **1998**; Chapter 8.

34. Podlech, J.; Seebach, D. *Helv. Chim. Acta.* **1995**, *78*, 1238-1246.

35. McKervey, M. A.; Dilworth, B .M.; Collins, J. C., unpublished work (see Dilworth, B. M., Ph.D. Thesis, NUI, 1987; Collins, J. C., Ph.D. Thesis, NUI, 1990).

36. Hruby, V. J.; Bonner, G. G. in *Methods in Molecular Biology*, *Vol. 35: Peptide*

Synthesis Protocols Pennington, M. M.; Dunn, B. M. Eds, Humana Press, New Jersey, 1994, p 201.

37. Kulkowit, S.; McKervey, M. A. *J. Chem. Soc., Chem. Commun.* **1981**, *14*, 616-617.

38. Gelb, M. H.; Lin, Y.; Pickard, M. A.; Song, Y.; Vederas, J. C. *J. Am. Chem. Soc.* **1990**, *112*, 4932-4942.

39. Baum, J. S.; Shook, D. A.; Davies, H. M. L.; Smith, H. D. *Synth. Commun.* **1987**, *17*, 1709-1714.

40. Hiebl, J.; Kollmann, H.; Rovenszky, F.; Winkler, K. *J. Org. Chem.* **1999**, *64*, 1947-1952.

41. Hanessian, S.; McNaughton-Smith, G.; Lombart, H. G.; Lubell, W. D. *Tetrahedron* **1997**, *53*, 12789-12854.

42. Kubasch, N.; Schmidt, R. R. *Eur. J. Org. Chem.* **2002**, *16*, 2710-2726.

43. (a) Williams, R. M. In *Synthesis of Optically Active α-Amino Acids, Vol. 7 of Organic Chemistry Series*; Baldwin, J. E.; Magnus, P. D., Eds.; Pergamon Prss: Oxford, 1989. (b) Duthaler, R. O. *Tetrahedron* **1994**, *50*, 1539-1650. (c) Cativiela, C.; Diaz-de-Villegas, M. D. *Tetrahedron:Asymmetry* **1998**, *9*, 3517-3599. (d) Cativiela, C.; Diaz-de-Villegas, M. D. *Tetrahedron:Asymmetry* **2000**, *11*, 645-732.

44. Gante, G. *Angew. Chem., Int. Ed. Engl.* **1994**, *33*, 1699-1730.

45. (a) Giannis, A.; Kolter, T. *Angew. Chem. Int. Ed. Engl.* **1993**, *32*, 1244. (b) Mendel, D.; Ellman, J.; Schultz, P. G. *J. Am. Chem. Soc.* **1993**, *115*, 4359-4360.

46. (a) Chamberlin, R.; Bridges, R. In *Drug Design for Neuroscience*; Lozikowski, A. P., Ed.; Raven Press: New York, 1993; p. 261; (b) Brown, P. *New Scientist* **1992**, *136*, 1.

47. (a) Belokon, Yu. N.; Chernoglazova, N. I.; Batsanov, A. S.; Garbalinskaya, N. S.; Bakhmutov, V. I.; Struchkov, Yu. T.; Belikov, V. M. *Izv. Akad. Nauk SSSR, Ser. Khim.* **1987**, *4*, 852-857. (b) Mulzer, J.; Schroder, F.; Lobbia, A.; Buschmann, J.; Luger, P. *Angew. Chem., Int. Ed. Engl.* **1994**, *33*, 1737-1739. (c) Avenoza, A.; Cativiela, C.; Peregrina, J. M.; Zurbano, M. M. *Tetrahedron: Asymmetry* **1996**, *7*, 1555-1558. (d) Avenoza, A.; Cativiela, C.; Peregrina, J. M.; Zurbano, M. M. *Tetrahedron: Asymmetry* **1997**, *8*, 863-871. (e) Tanaka, K.; Sawanishi H. *Tetrahedron: Asymmetry* **2000**, *11*, 3837-3843. (f) Kabat, M. M. *Tetrahedron Lett.* **2001**, *42*, 7521-7524. (g) Yang, M. M. Unpublished work in our laboratory.

48. (a) Goldman, P. *Science* **1969**, *164*, 1123. (b) Smith, F. A. *Chem. Tech.* **1973**, 422. (c) Filler, R. *Chem. Tech.* **1974**, 752. (d) *Ciba Foundation Symposium, Carbon-Fluorine Compounds, Chemistry, Biochemistry and Biological Activities.* Elsevier, New York 1972. (e) Filler, R. in *Organofluorine Chemicals and Their Industrial Applications* (ed. R. F. Banks and E. Horwood). Halsted, New York, 1979. (f) *Biomedical Aspects of Fluorine Chemistry* (ed. R. Filler and Y. Kobayashi). Kodansha Ltd., Tokyo 1982. (g) *Biochemistry Involving Carbon-Fluorine Bonds* (ed. R. Filler). American Chemistry Society, Washington 1976. (h) Gerstenberger, M. R. C.; Haas, A. *Angew. Chem. Int. Ed.* **1981**, *20*, 647.

49. Welch, J. T. *Tetrahedron* **1987**, *43*, 3123-3197.

50. Andrews, M. J. I.; Tabor, A. B. *Tetrahedron Lett.* **1997**, *38*, 3063-3066.

51. Kollonitsch, J.; Perkins, L. M.; Patchett, A. A.; Doldouras, G. A.; Marburg, S.; Duggan, D. E.; Maycock, A. L.; Aster, S. D. *Nature* **1978**, *274*, 906.

52. (a) Regitz, M. *Angew. Chem. Int. Ed. Engl.* **1976**, *6*, 733-734. (b) Regitz, M. *Synthesis* **1972**, 351-353. (c) Regitz, M.; Maas, G. *Diazo Compounds: Properties and Synthesis*; Academic Press, Orlando, 1986 Chapter 13.

53. Baum, J. S.; Shook, D. A.; Davies, H. M. L.; Smith, H. D. *Synth. Commun.* **1987**, *17*, 1709-1714.

54. Studer, M.; Burkhardt, S.; Indolese, A. F.; Blaser H. U. *J. Chem. Soc., Chem. Commun.* **2000**, *14*, 1327-1328.

55. Musher, J. I. *Angew. Chem. Intl. Ed. Engl.* **1969**, *8*, 54.

56. (a) Pimentel, G. C. *J. Chem. Phys.* **1951**, *19*, 446. (b) Hach, R. J.; Rundle, R. E. *J. Am. Chem. Soc.* **1951**, *73*, 4321-4324.

57. Hayes, R. A.; Martin, J. C. *"Studies in Organic Chemistry"* Vol. 19, *Organic Sulfur Chemistry*, Chapter 8, Elsevier, **1985**.

58. Lee, D.Y.; Martin, J. C. *J. Am. Chem. Soc.* **1984**, *106*, 5745-.

59. Yamashita, M.; Yamamoto, Y.; Akiba, K.; Hashizume, D.; Iwasaki, F.; Nagase, S. *J. Am. Chem. Soc.* **2005**, *127*, 4354-4371.

60. Ault, B. S.; Andrews, L. *J. Am. Chem. Soc.* **1976**, *98*, 1591.

61. Wada, M.; Kanzaki M.; Ogura H.; Hayase S.; Erabi T. *J. Organomet. Chem.* **1995**,*485*, 127-133.

62. Senear, A. E.; Valient, W.; Wirth, J. *J. Org. Chem.* **1960**, *25*, 2001-2006.

63. McOmie, J. F. W.; Watts, M. L.; West, D. E. *Tetrahedron* **1968**, *24*, 2289-2292.

64. Olah, G. A.; Narang, S. C.; Balaram-Gupta, B. G.; Malhota, R. *J. Am. Chem. Soc.* **1979**, *44*, 1247.

65. Frye, C. L.; Vincent, G. A.; Hauschildt, G. L. *J. Am. Chem. Soc.* **1966**, *88*, 2727.

66. Mottier, M. *Helv. Chim. Acta.* **1935**, *18*, 840.

67. Cameron, M.; Wilson, R. D. *Applied Catalysis A: General* **2000**, *203*, 307-310.

68. Dunbar, K. R.; Quillevere, A. *Polyhedron* **1993**, *12*, 807.

69. Dunbar, K. R.; Quillevere, A. *Angew. Chem., Int. Ed.* **1993**, *32*, 293.

70. (a) Bricklebank, N.; Godfrey, S. M.; McAuliffe, C. A.; Pritchard, R. G. *Acta Crystallogr., Sect. C: Cryst. Struct. Commun.* **1993**, *49,* 1017. (b) Hiemisch, O.; Henschel, D.; Jones, P. G.; Blaschette, A. *Z. Anorg. Allg. Chem.* **1996**, *622*, 829. (C) Burke, J. M.; Fox, M. A.; Goeta, A. E.; Hughes, A. K.; Marder, T. B. *Chem. Commun.* **2000**, 2217. (d) Majeste, R. J.; Chriss, D.; Trefonas, L. M. *Inorg. Chem.* **1977**, *16*, 188. (e) Ershova, M. M.; Glushkova, M. A.; Chumaevskii, N. A.; Prai-Koshits, M. A.; Buslaev, Yu. A.; Butman, L. A.; Minaeva, N. A.; Sadikov, G. G. *Koord. Khim. (Russ.) (Coord. Chem.)* **1981**, *7*, 556. (f) McGrath, T. D.; Welch, A. J. *Acta Crystallogr., Sect. C: Cryst. Struct. Commun.* **1997**, *53*, 229. (g) Baker, P.K.; Meehan, M. M.; Metcalfe,

T.; Drew, M. G. B. *Gazz. Chim. Ital.* **1997**, *127*, 217. (h) hasselgren, C.; Dean, P. A. W.; Scudder, M. L.; Craig, D. C.; Dance, I. G. *J. Chem. Soc., Dalton Trans.* **1997**, 2019. (i) Junk, P. C.; Atwood, J. L. *J. Coord. Chem.* **1999**, *46*, 505. (j) Robinson, P. D.; Hinckley, C. C.; Matusz, M.; Kibala, P. A. *Acta Crystallogr., Sect. C: Cryst. Struct. Commun.* **1988**, *44*, 619. (k) Khan, M. A.; Tuck, D. G.; Taylor, M. J.; Rogers, D. A. *J. Crystallogr. Spectrosc. Res.* **1986**, *16*, 895.

71. Schmutzler, R.; Schomburg, D.; Bartsch, R.; Stelzer, O. *Z. Naturforsch., B: Chem. Sci.* **1984**, *39*, 1177.

72. Livant, P. D.; Northcott, D. J. D.; Shen, Y.; Webb, T. R. *J. Org. Chem.* **2004**, *69*, 6564-6571.

73. Li, H. *Syntheses of Possible Precursors to 10-P-5 and 10-N-5 Species*, M. S. Thesis, Auburn University, **1999**.

74. Inguimbert, N.; Dhôtel, H.; Coric, P.; Roques, B. P. *Tetrahedron Lett.* **2005**, *46*, 3517-3520.

75. (a) Koech, P. K.; Krische, M. J. *Org. Lett.* **2004**, *6(5)*, 691-694. (b) Huddleston, R. R.; Krische, M. J. *Org. Lett.* **2003**, *5(7)*, 1143-1146.

APPENDICES

Appendix A. Crystal structure data (CIF file) for compound **44**.

data_face

_audit_creation_method   SHELXL-97
_chemical_name_systematic
;
 ?
;
_chemical_name_common   ?
_chemical_melting_point   ?
_chemical_formula_moiety   ?
_chemical_formula_sum
 'C7 H11 N1 O5'
_chemical_formula_weight   756.67

loop_
  _atom_type_symbol
  _atom_type_description
  _atom_type_scat_dispersion_real
  _atom_type_scat_dispersion_imag
  _atom_type_scat_source
 'C'   'C'   0.0033   0.0016
 'International Tables Vol C Tables 4.2.6.8 and 6.1.1.4'
 'H'   'H'   0.0000   0.0000
 'International Tables Vol C Tables 4.2.6.8 and 6.1.1.4'
 'N'   'N'   0.0061   0.0033
 'International Tables Vol C Tables 4.2.6.8 and 6.1.1.4'
 'O'   'O'   0.0106   0.0060
 'International Tables Vol C Tables 4.2.6.8 and 6.1.1.4'

_symmetry_cell_setting   'orthorhombic'
_symmetry_space_group_name_H-M   'P2(1)2(1)2(1)'

loop_
  _symmetry_equiv_pos_as_xyz
 'x, y, z'
 '-x+1/2, -y, z+1/2'

```
 '-x, y+1/2, -z+1/2'
 'x+1/2, -y+1/2, -z
_cell_length_a                      5.0678(5)
_cell_length_b                      11.2996(10)
_cell_length_c                      16.1160(15)
_cell_angle_alpha                   90.00
_cell_angle_beta                    90.00
_cell_angle_gamma                    90.00
_cell_volume                         922.87(15)
_cell_formula_units_Z                4
_cell_measurement_temperature        193(2)
_cell_measurement_reflns_used       9416
_cell_measurement_theta_min         2.20
_cell_measurement_theta_max         28.36

_exptl_crystal_description          'prism'
_exptl_crystal_colour                'colorless'
_exptl_crystal_size_max             .700
_exptl_crystal_size_mid             .100
_exptl_crystal_size_min              .100
_exptl_crystal_density_meas         'not measured'
_exptl_crystal_density_diffrn       1.361
_exptl_crystal_density_method        'not measured'
_exptl_crystal_F_000                 400
_exptl_absorpt_coefficient_mu       0.117
_exptl_absorpt_correction_type      'numerical'
_exptl_absorpt_correction_T_min     0.95836
_exptl_absorpt_correction_T_max      0.98905
_exptl_absorpt_process_details      'SADABS'

_exptl_special_details
;
 ?
;

_diffrn_ambient_temperature          193(2)
_diffrn_radiation_wavelength        0.71073
_diffrn_radiation_type               MoK\a
_diffrn_radiation_source            'fine-focus sealed tube'
_diffrn_radiation_monochromator      graphite
_diffrn_measurement_device_type      'Bruker APEX'
_diffrn_measurement_method             '0.3 wide w/ exposures'
_diffrn_detector_area_resol_mean    0
_diffrn_standards_number             'na'
_diffrn_standards_interval_count    'na'
_diffrn_standards_interval_time      'na'
```

_diffrn_standards_decay_%   0
_diffrn_reflns_number   9366
_diffrn_reflns_av_R_equivalents   0.0321
_diffrn_reflns_av_sigmaI/netI   0.0281
_diffrn_reflns_limit_h_min   -6
_diffrn_reflns_limit_h_max   6
_diffrn_reflns_limit_k_min   -15
_diffrn_reflns_limit_k_max   15
_diffrn_reflns_limit_l_min   -21
_diffrn_reflns_limit_l_max   20
_diffrn_reflns_theta_min   2.20
_diffrn_reflns_theta_max   28.36
_reflns_number_total   2297
_reflns_number_gt   2042
_reflns_threshold_expression   >2sigma(I)

_computing_data_collection   'SMART'
_computing_cell_refinement   'SMART,   SAINT'
_computing_data_reduction   'SAINT'
_computing_structure_solution   'SHELXS-97 (Sheldrick, 1990)'
_computing_structure_refinement   'SHELXL-97 (Sheldrick, 1997)'
_computing_molecular_graphics   'SHELXP-97 (Sheldrick, 1997)'
_computing_publication_material   'SHELXCIF-97 (Sheldrick, 2000)'

_refine_special_details
;
Refinement of F^2^ against ALL reflections.   The weighted R-factor wR and
goodness of fit S are based on F^2^, conventional R-factors R are based
on F, with F set to zero for negative F^2^. The threshold expression of
F^2^ > 2sigma(F^2^) is used only for calculating R-factors(gt) etc. and is
not relevant to the choice of reflections for refinement.   R-factors based
on F^2^ are statistically about twice as large as those based on F, and R-
factors based on ALL data will be even larger.
;

_refine_ls_structure_factor_coef   Fsqd
_refine_ls_matrix_type   full
_refine_ls_weighting_scheme   calc
_refine_ls_weighting_details
'calc w=1/[\s^2^(Fo^2^)+(0.0752P)^2^+0.0097P] where P=(Fo^2^+2Fc^2^)/3'
_atom_sites_solution_primary   direct
_atom_sites_solution_secondary   difmap
_atom_sites_solution_hydrogens   geom
_refine_ls_hydrogen_treatment   mixed
_refine_ls_extinction_method   none
_refine_ls_extinction_coef   ?

_refine_ls_abs_structure_details
 'Flack H D (1983), Acta Cryst. A39, 876-881'
_refine_ls_abs_structure_Flack   0.3(12)
_refine_ls_number_reflns   2297
_refine_ls_number_parameters   118
_refine_ls_number_restraints   0
_refine_ls_R_factor_all   0.0476
_refine_ls_R_factor_gt   0.0429
_refine_ls_wR_factor_ref   0.1136
_refine_ls_wR_factor_gt   0.1115
_refine_ls_goodness_of_fit_ref   1.049
_refine_ls_restrained_S_all   1.049
_refine_ls_shift/su_max   0.001
_refine_ls_shift/su_mean   0.000

loop_
  _atom_site_label
  _atom_site_type_symbol
  _atom_site_fract_x
  _atom_site_fract_y
  _atom_site_fract_z
  _atom_site_U_iso_or_equiv
  _atom_site_adp_type
  _atom_site_occupancy
  _atom_site_symmetry_multiplicity
  _atom_site_calc_flag
  _atom_site_refinement_flags
  _atom_site_disorder_assembly
  _atom_site_disorder_group
C4 C -0.0009(4) 0.59200(13) 0.81987(10) 0.0319(3) Uani 1 1 d . . .
O1 O 0.0052(3) 0.59020(10) 1.11748(7) 0.0391(3) Uani 1 1 d . . .
C1 C 0.1480(3) 0.61401(12) 1.05091(10) 0.0269(3) Uani 1 1 d . . .
C3 C 0.1634(3) 0.60757(13) 0.89644(10) 0.0279(3) Uani 1 1 d . . .
H3A H 0.2089 0.6923 0.9030 0.033 Uiso 1 1 calc R . .
H3B H 0.3299 0.5626 0.8903 0.033 Uiso 1 1 calc R . .
O2 O 0.1083(3) 0.64643(14) 0.75549(7) 0.0491(4) Uani 1 1 d . . .
C5 C -0.0324(6) 0.6382(2) 0.67762(12) 0.0630(6) Uani 1 1 d . . .
H5A H 0.0646 0.6816 0.6347 0.094 Uiso 1 1 calc R . .
H5B H -0.2088 0.6726 0.6840 0.094 Uiso 1 1 calc R . .
H5C H -0.0484 0.5549 0.6614 0.094 Uiso 1 1 calc R . .
C6 C 0.1031(4) 0.63393(17) 1.19590(11) 0.0452(4) Uani 1 1 d . . .
H6A H -0.0179 0.6105 1.2404 0.068 Uiso 1 1 calc R . .
H6B H 0.1153 0.7204 1.1938 0.068 Uiso 1 1 calc R . .
H6C H 0.2782 0.6005 1.2066 0.068 Uiso 1 1 calc R . .
O4 O 0.3522(3) 0.66760(13) 1.05216(8) 0.0478(4) Uani 1 1 d . . .
C7 C 0.0245(3) 0.43010(11) 0.98115(9) 0.0224(3) Uani 1 1 d . . .

O3 O -0.2041(3) 0.53906(16) 0.81592(8) 0.0559(4) Uani 1 1 d . . .
C2 C 0.0179(3) 0.56488(11) 0.97361(8) 0.0227(3) Uani 1 1 d . . .
H2A H -0.1696 0.5922 0.9713 0.027 Uiso 1 1 calc R . .
O5 O 0.24075(19) 0.37986(9) 0.98167(9) 0.0345(3) Uani 1 1 d . . .
N1 N -0.2005(2) 0.37440(11) 0.98872(9) 0.0295(3) Uani 1 1 d . . .
H1A H -0.2028 0.2970 0.9946 0.035 Uiso 1 1 calc R . .
H1B H -0.3495 0.4144 0.9880 0.035 Uiso 1 1 calc R . .

loop_
  _atom_site_aniso_label
  _atom_site_aniso_U_11
  _atom_site_aniso_U_22
  _atom_site_aniso_U_33
  _atom_site_aniso_U_23
  _atom_site_aniso_U_13
  _atom_site_aniso_U_12
C4 0.0338(8) 0.0317(7) 0.0301(7) 0.0003(5) 0.0030(7) 0.0076(7)
O1 0.0437(7) 0.0430(6) 0.0305(6) -0.0058(4) 0.0011(5) -0.0132(6)
C1 0.0281(7) 0.0195(6) 0.0330(7) 0.0015(5) -0.0038(6) -0.0002(5)
C3 0.0262(7) 0.0250(7) 0.0325(7) 0.0032(6) 0.0022(6) -0.0012(6)
O2 0.0593(9) 0.0562(8) 0.0319(6) 0.0092(6) 0.0019(6) -0.0044(7)
C5 0.0833(17) 0.0782(14) 0.0275(9) 0.0073(9) -0.0005(9) 0.0111(14)
C6 0.0591(12) 0.0450(10) 0.0316(8) -0.0056(7) -0.0023(8) -0.0069(9)
O4 0.0435(8) 0.0570(8) 0.0430(7) -0.0002(6) -0.0051(6) -0.0242(7)
C7 0.0199(6) 0.0199(5) 0.0275(6) 0.0005(5) -0.0005(6) 0.0006(5)
O3 0.0470(8) 0.0825(11) 0.0381(7) 0.0015(7) -0.0084(6) -0.0213(8)
C2 0.0187(6) 0.0199(5) 0.0294(7) 0.0005(5) -0.0006(6) 0.0003(5)
O5 0.0185(5) 0.0220(5) 0.0630(7) 0.0038(5) 0.0009(5) 0.0016(4)
N1 0.0196(6) 0.0207(6) 0.0481(8) 0.0020(5) -0.0001(5) 0.0001(4)

_geom_special_details
;
  All esds (except the esd in the dihedral angle between two l.s. planes)
  are estimated using the full covariance matrix.   The cell esds are taken
  into account individually in the estimation of esds in distances, angles
  and torsion angles; correlations between esds in cell parameters are only
  used when they are defined by crystal symmetry.   An approximate (isotropic)
  treatment of cell esds is used for estimating esds involving l.s. planes.
;

loop_
  _geom_bond_atom_site_label_1
  _geom_bond_atom_site_label_2
  _geom_bond_distance
  _geom_bond_site_symmetry_2
  _geom_bond_publ_flag
74

C4 O3 1.193(2) . ?
C4 O2 1.327(2) . ?
C4 C3 1.499(2) . ?
O1 C1 1.322(2) . ?
O1 C6 1.445(2) . ?
C1 O4 1.199(2) . ?
C1 C2 1.515(2) . ?
C3 C2 1.524(2) . ?
O2 C5 1.446(3) . ?
C7 O5 1.2344(16) . ?
C7 N1 1.3079(18) . ?
C7 C2 1.5281(17) . ?

loop_
  _geom_angle_atom_site_label_1
  _geom_angle_atom_site_label_2
  _geom_angle_atom_site_label_3
  _geom_angle
  _geom_angle_site_symmetry_1
  _geom_angle_site_symmetry_3
  _geom_angle_publ_flag
O3 C4 O2 123.42(16) . . ?
O3 C4 C3 125.63(15) . . ?
O2 C4 C3 110.95(15) . . ?
C1 O1 C6 116.90(14) . . ?
O4 C1 O1 124.17(14) . . ?
O4 C1 C2 125.06(14) . . ?
O1 C1 C2 110.77(12) . . ?
C4 C3 C2 111.45(13) . . ?
C4 O2 C5 116.30(18) . . ?
O5 C7 N1 123.51(11) . . ?
O5 C7 C2 118.57(12) . . ?
N1 C7 C2 117.90(12) . . ?
C1 C2 C3 110.14(12) . . ?
C1 C2 C7 106.87(11) . . ?
C3 C2 C7 111.70(12) . . ?

_diffrn_measured_fraction_theta_max   0.992
_diffrn_reflns_theta_full   28.36
_diffrn_measured_fraction_theta_full   0.992
_refine_diff_density_max   0.372
_refine_diff_density_min   -0.159
_refine_diff_density_rms   0.049

Appendix B. Crystal structure data (CIF file) for compound **63**.

data_p21n

_audit_creation_method   SHELXL-97
_chemical_name_systematic
;
 ?
;
_chemical_name_common   ?
_chemical_melting_point   ?
_chemical_formula_moiety   ?
_chemical_formula_sum
 'C22 H26 Cl O7 P'
_chemical_formula_weight   468.85

loop_
 _atom_type_symbol
 _atom_type_description
 _atom_type_scat_dispersion_real
 _atom_type_scat_dispersion_imag
 _atom_type_scat_source
 'C' 'C'   0.0033   0.0016
 'International Tables Vol C Tables 4.2.6.8 and 6.1.1.4'
 'H' 'H'   0.0000   0.0000
 'International Tables Vol C Tables 4.2.6.8 and 6.1.1.4'
 'O' 'O'   0.0106   0.0060
 'International Tables Vol C Tables 4.2.6.8 and 6.1.1.4'
 'P' 'P'   0.1023   0.0942
 'International Tables Vol C Tables 4.2.6.8 and 6.1.1.4'
 'Cl' 'Cl'   0.1484   0.1585
 'International Tables Vol C Tables 4.2.6.8 and 6.1.1.4'

_symmetry_cell_setting   ?

_symmetry_space_group_name_H-M   ?

loop_
 _symmetry_equiv_pos_as_xyz
 'x, y, z'
 '-x+1/2, y+1/2, -z+1/2'
 '-x, -y, -z'
 'x-1/2, -y-1/2, z-1/2'

_cell_length_a   8.9250(10)
_cell_length_b   17.926(2)
_cell_length_c   14.692(2)
_cell_angle_alpha   90.000(2)
_cell_angle_beta   100.157(2)
_cell_angle_gamma   90.000(2)
_cell_volume   2313.7(5)
_cell_formula_units_Z   4
_cell_measurement_temperature   193(2)
_cell_measurement_reflns_used   ?
_cell_measurement_theta_min   ?
_cell_measurement_theta_max   ?

_exptl_crystal_description   ?
_exptl_crystal_colour   ?
_exptl_crystal_size_max   ?
_exptl_crystal_size_mid   ?
_exptl_crystal_size_min   ?
_exptl_crystal_density_meas   ?
_exptl_crystal_density_diffrn   1.346
_exptl_crystal_density_method   'not measured'
_exptl_crystal_F_000   984
_exptl_absorpt_coefficient_mu   0.274
_exptl_absorpt_correction_type   ?
_exptl_absorpt_correction_T_min   ?
_exptl_absorpt_correction_T_max   ?
_exptl_absorpt_process_details   ?

_exptl_special_details
;
 ?
;

_diffrn_ambient_temperature   193(2)
_diffrn_radiation_wavelength   0.71073
_diffrn_radiation_type   MoK\a
_diffrn_radiation_source   'fine-focus sealed tube'

```
_diffrn_radiation_monochromator      graphite
_diffrn_measurement_device_type      ?
_diffrn_measurement_method             ?
_diffrn_detector_area_resol_mean   ?
_diffrn_standards_number               ?
_diffrn_standards_interval_count   ?
_diffrn_standards_interval_time    ?
_diffrn_standards_decay_%              ?
_diffrn_reflns_number                23442
_diffrn_reflns_av_R_equivalents    0.0844
_diffrn_reflns_av_sigmaI/netI      0.0826
_diffrn_reflns_limit_h_min          -11
_diffrn_reflns_limit_h_max           11
_diffrn_reflns_limit_k_min          -23
_diffrn_reflns_limit_k_max           23
_diffrn_reflns_limit_l_min          -19
_diffrn_reflns_limit_l_max           19
_diffrn_reflns_theta_min            2.27
_diffrn_reflns_theta_max            28.35
_reflns_number_total                 5738
_reflns_number_gt                     3213
_reflns_threshold_expression        >2sigma(I)

_computing_data_collection             ?
_computing_cell_refinement             ?
_computing_data_reduction              ?
_computing_structure_solution       'SHELXS-97 (Sheldrick, 1990)'
_computing_structure_refinement     'SHELXL-97 (Sheldrick, 1997)'
_computing_molecular_graphics          ?
_computing_publication_material     ?

_refine_special_details
;
 Refinement of F^2^ against ALL reflections.   The weighted R-factor wR and
 goodness of fit S are based on F^2^, conventional R-factors R are based
 on F, with F set to zero for negative F^2^. The threshold expression of
 F^2^ > 2sigma(F^2^) is used only for calculating R-factors(gt) etc. and is
 not relevant to the choice of reflections for refinement.   R-factors based
 on F^2^ are statistically about twice as large as those based on F, and R-
 factors based on ALL data will be even larger.
;

_refine_ls_structure_factor_coef   Fsqd
_refine_ls_matrix_type                full
_refine_ls_weighting_scheme           calc
_refine_ls_weighting_details
```

'calc w=1/[\s^2^(Fo^2^)+(0.0831P)^2^+0.0000P] where P=(Fo^2^+2Fc^2^)/3'
_atom_sites_solution_primary   direct
_atom_sites_solution_secondary   difmap
_atom_sites_solution_hydrogens   geom
_refine_ls_hydrogen_treatment   mixed
_refine_ls_extinction_method   none
_refine_ls_extinction_coef   ?
_refine_ls_number_reflns   5738
_refine_ls_number_parameters   288
_refine_ls_number_restraints   0
_refine_ls_R_factor_all   0.1032
_refine_ls_R_factor_gt   0.0587
_refine_ls_wR_factor_ref   0.1575
_refine_ls_wR_factor_gt   0.1436
_refine_ls_goodness_of_fit_ref   0.903
_refine_ls_restrained_S_all   0.903
_refine_ls_shift/su_max   0.076
_refine_ls_shift/su_mean   0.009

loop_
  _atom_site_label
  _atom_site_type_symbol
  _atom_site_fract_x
  _atom_site_fract_y
  _atom_site_fract_z
  _atom_site_U_iso_or_equiv
  _atom_site_adp_type
  _atom_site_occupancy
  _atom_site_symmetry_multiplicity
  _atom_site_calc_flag
  _atom_site_refinement_flags
  _atom_site_disorder_assembly
  _atom_site_disorder_group
P1 P 0.65162(7) 0.08868(4) 0.25817(5) 0.03365(19) Uani 1 1 d . . .
Cl1 Cl 0.82487(8) 0.12525(4) 0.65688(5) 0.0484(2) Uani 1 1 d . . .
O1 O 0.4273(2) -0.02282(10) 0.27741(15) 0.0565(6) Uani 1 1 d . . .
H1A H 0.3615 -0.0546 0.2850 0.085 Uiso 1 1 calc R . .
O2 O 0.4744(2) 0.22340(12) 0.17898(15) 0.0519(5) Uani 1 1 d . . .
O3 O 0.8746(2) -0.02842(11) 0.28779(13) 0.0522(5) Uani 1 1 d . . .
H3A H 0.9348 -0.0648 0.2963 0.078 Uiso 1 1 calc R . .
O4 O 0.5780(2) 0.11216(11) 0.04688(13) 0.0524(5) Uani 1 1 d . . .
H4A H 0.6159 0.1522 0.0701 0.079 Uiso 1 1 calc R . .
O5 O 0.7826(2) 0.20697(10) 0.14906(12) 0.0457(5) Uani 1 1 d . . .
H5B H 0.8002 0.2452 0.1196 0.069 Uiso 1 1 calc R . .
O6 O 0.7182(3) 0.13404(12) 0.44566(14) 0.0638(6) Uani 1 1 d . . .
H6A H 0.7381 0.1468 0.5015 0.096 Uiso 1 1 calc R . .

O7 O 0.8237(3) 0.31142(13) 0.02966(16) 0.0811(8) Uani 1 1 d . . .
C1 C 0.4502(3) 0.10155(14) 0.23108(17) 0.0336(6) Uani 1 1 d . . .
C2 C 0.3575(3) 0.04219(15) 0.24746(19) 0.0412(6) Uani 1 1 d . . .
C3 C 0.2019(3) 0.05056(16) 0.2328(2) 0.0530(8) Uani 1 1 d . . .
H3B H 0.1387 0.0102 0.2442 0.064 Uiso 1 1 calc R . .
C4 C 0.1383(3) 0.11798(17) 0.2014(2) 0.0538(8) Uani 1 1 d . . .
H4B H 0.0308 0.1235 0.1917 0.065 Uiso 1 1 calc R . .
C5 C 0.2254(3) 0.17673(16) 0.1841(2) 0.0452(7) Uani 1 1 d . . .
H5A H 0.1792 0.2227 0.1625 0.054 Uiso 1 1 calc R . .
C6 C 0.3814(3) 0.16895(14) 0.19835(18) 0.0366(6) Uani 1 1 d . . .
C7 C 0.7235(3) 0.04039(14) 0.17002(17) 0.0350(6) Uani 1 1 d . . .
C8 C 0.8257(3) -0.01864(14) 0.1955(2) 0.0408(6) Uani 1 1 d . . .
C9 C 0.8724(4) -0.06228(17) 0.1298(2) 0.0564(8) Uani 1 1 d . . .
H9A H 0.9419 -0.1020 0.1474 0.068 Uiso 1 1 calc R . .
C10 C 0.8187(4) -0.0484(2) 0.0384(2) 0.0697(10) Uani 1 1 d . . .
H10A H 0.8494 -0.0801 -0.0069 0.084 Uiso 1 1 calc R . .
C11 C 0.7212(4) 0.01013(19) 0.0097(2) 0.0590(9) Uani 1 1 d . . .
H11A H 0.6870 0.0195 -0.0542 0.071 Uiso 1 1 calc R . .
C12 C 0.6750(3) 0.05442(15) 0.07568(19) 0.0427(7) Uani 1 1 d . . .
C13 C 0.7529(3) 0.17063(14) 0.29833(17) 0.0372(6) Uani 1 1 d . . .
C14 C 0.8077(3) 0.22225(14) 0.24043(18) 0.0389(6) Uani 1 1 d . . .
C15 C 0.8841(3) 0.28535(16) 0.2765(2) 0.0519(8) Uani 1 1 d . . .
H15A H 0.9213 0.3202 0.2371 0.062 Uiso 1 1 calc R . .
C16 C 0.9059(4) 0.29722(18) 0.3701(2) 0.0621(9) Uani 1 1 d . . .
H16A H 0.9584 0.3408 0.3949 0.075 Uiso 1 1 calc R . .
C17 C 0.8537(4) 0.24782(19) 0.4291(2) 0.0580(8) Uani 1 1 d . . .
H17A H 0.8704 0.2572 0.4938 0.070 Uiso 1 1 calc R . .
C18 C 0.7772(3) 0.18478(17) 0.39356(19) 0.0460(7) Uani 1 1 d . . .
C19 C 0.8840(6) 0.2144(3) -0.0659(3) 0.123(2) Uani 1 1 d . . .
H19A H 0.8843 0.2013 -0.1306 0.185 Uiso 1 1 calc R . .
H19B H 0.8186 0.1796 -0.0395 0.185 Uiso 1 1 calc R . .
H19C H 0.9880 0.2116 -0.0308 0.185 Uiso 1 1 calc R . .
C20 C 0.8277(6) 0.2881(3) -0.0612(3) 0.1070(16) Uani 1 1 d . . .
H20A H 0.8928 0.3228 -0.0893 0.128 Uiso 1 1 calc R . .

H20B H 0.7236 0.2908 -0.0979 0.128 Uiso 1 1 calc R . .
C21 C 0.7751(12) 0.3857(3) 0.0364(4) 0.207(5) Uani 1 1 d . . .
H21A H 0.7296 0.3834 0.0931 0.248 Uiso 1 1 calc R . .
H21B H 0.8734 0.4117 0.0558 0.248 Uiso 1 1 calc R . .
C22 C 0.7079(16) 0.4288(4) -0.0020(5) 0.321(8) Uani 1 1 d . . .
H22A H 0.7102 0.4736 0.0364 0.481 Uiso 1 1 calc R . .
H22B H 0.6026 0.4115 -0.0197 0.481 Uiso 1 1 calc R . .
H22C H 0.7495 0.4405 -0.0578 0.481 Uiso 1 1 calc R . .
H1 H 0.672(3) 0.0434(13) 0.3259(17) 0.038(7) Uiso 1 1 d . . .
H2A H 0.434(4) 0.268(2) 0.175(3) 0.087(12) Uiso 1 1 d . . .

```
loop_
  _atom_site_aniso_label
  _atom_site_aniso_U_11
  _atom_site_aniso_U_22
  _atom_site_aniso_U_33
  _atom_site_aniso_U_23
  _atom_site_aniso_U_13
  _atom_site_aniso_U_12
P1 0.0326(4) 0.0367(4) 0.0305(4) 0.0024(3) 0.0023(3) 0.0011(3)
Cl1 0.0556(5) 0.0414(4) 0.0453(4) 0.0057(3) 0.0012(3) -0.0025(3)
O1 0.0419(12) 0.0415(11) 0.0836(16) 0.0181(10) 0.0039(11) -0.0007(9)
O2 0.0418(12) 0.0408(11) 0.0712(15) 0.0148(10) 0.0051(10) 0.0027(10)
O3 0.0505(12) 0.0556(12) 0.0494(13) 0.0102(10) 0.0055(10) 0.0186(10)
O4 0.0531(12) 0.0578(12) 0.0397(11) 0.0020(9) -0.0097(9) 0.0029(10)
O5 0.0554(12) 0.0489(11) 0.0328(10) 0.0009(8) 0.0076(9) -0.0081(9)
O6 0.0867(17) 0.0733(15) 0.0305(11) -0.0037(10) 0.0079(11) -0.0179(13)
O7 0.143(2) 0.0575(14) 0.0476(14) 0.0038(11) 0.0293(15) -0.0024(15)
C1 0.0291(13) 0.0396(14) 0.0313(13) -0.0001(11) 0.0034(10) -0.0001(11)
C2 0.0372(15) 0.0430(15) 0.0425(16) 0.0030(12) 0.0049(12) 0.0039(12)
C3 0.0363(16) 0.0519(18) 0.070(2) 0.0124(16) 0.0070(15) -0.0065(14)
C4 0.0287(15) 0.065(2) 0.066(2) 0.0069(16) 0.0040(14) 0.0033(14)
C5 0.0382(16) 0.0448(16) 0.0507(17) 0.0026(13) 0.0023(13) 0.0085(13)
C6 0.0367(15) 0.0371(14) 0.0361(15) -0.0014(11) 0.0061(12) 0.0014(12)
C7 0.0323(14) 0.0380(14) 0.0339(14) -0.0025(11) 0.0036(11) -0.0038(11)
C8 0.0360(15) 0.0384(14) 0.0475(17) 0.0005(12) 0.0059(13) -0.0038(12)
C9 0.057(2) 0.0498(18) 0.062(2) -0.0105(16) 0.0090(16) 0.0122(15)
C10 0.080(2) 0.068(2) 0.062(2) -0.0288(19) 0.0163(19) 0.0061(19)
C11 0.068(2) 0.070(2) 0.0361(17) -0.0135(15) 0.0017(15) -0.0012(17)
C12 0.0402(16) 0.0461(16) 0.0398(16) -0.0035(13) 0.0015(12) -0.0048(13)
C13 0.0336(14) 0.0424(15) 0.0336(14) -0.0030(11) 0.0002(11) 0.0014(11)
C14 0.0337(14) 0.0454(15) 0.0361(15) -0.0017(12) 0.0019(12) 0.0021(12)
C15 0.0575(19) 0.0466(17) 0.0491(18) -0.0012(14) 0.0022(15) -0.0121(14)
C16 0.066(2) 0.0556(19) 0.057(2) -0.0094(16) -0.0087(17) -0.0156(17)
C17 0.066(2) 0.066(2) 0.0353(17) -0.0080(15) -0.0083(15) -0.0064(17)
C18 0.0445(17) 0.0567(18) 0.0346(16) -0.0012(13) 0.0006(13) -0.0006(14)
C19 0.190(6) 0.109(4) 0.087(3) 0.007(3) 0.069(4) 0.058(4)
C20 0.166(5) 0.103(4) 0.059(3) -0.002(2) 0.039(3) 0.012(3)
C21 0.435(14) 0.100(4) 0.089(4) 0.018(3) 0.058(6) 0.115(7)
C22 0.74(2) 0.151(7) 0.068(4) 0.010(4) 0.050(8) 0.196(11)

_geom_special_details
;
 All esds (except the esd in the dihedral angle between two l.s. planes)
 are estimated using the full covariance matrix.    The cell esds are taken
 into account individually in the estimation of esds in distances, angles
 and torsion angles; correlations between esds in cell parameters are only
```

used when they are defined by crystal symmetry.   An approximate (isotropic)
treatment of cell esds is used for estimating esds involving l.s. planes.
;

loop_
  _geom_bond_atom_site_label_1
  _geom_bond_atom_site_label_2
  _geom_bond_distance
  _geom_bond_site_symmetry_2
  _geom_bond_publ_flag
P1 C13 1.770(3) . ?
P1 C7 1.770(3) . ?
P1 C1 1.786(2) . ?
O1 C2 1.358(3) . ?
O2 C6 1.344(3) . ?
O3 C8 1.360(3) . ?
O4 C12 1.368(3) . ?
O5 C14 1.349(3) . ?
O6 C18 1.354(3) . ?
O7 C21 1.409(6) . ?
O7 C20 1.405(4) . ?
C1 C2 1.395(4) . ?
C1 C6 1.401(3) . ?
C2 C3 1.376(4) . ?
C3 C4 1.379(4) . ?
C4 C5 1.359(4) . ?
C5 C6 1.379(4) . ?
C7 C8 1.404(4) . ?
C7 C12 1.400(4) . ?
C8 C9 1.364(4) . ?
C9 C10 1.367(5) . ?
C10 C11 1.381(5) . ?
C11 C12 1.371(4) . ?
C13 C14 1.402(4) . ?
C13 C18 1.401(4) . ?
C14 C15 1.378(4) . ?
C15 C16 1.371(4) . ?
C16 C17 1.377(4) . ?
C17 C18 1.375(4) . ?
C19 C20 1.420(5) . ?
C21 C22 1.075(8) . ?

loop_
  _geom_angle_atom_site_label_1
  _geom_angle_atom_site_label_2
  _geom_angle_atom_site_label_3

_geom_angle
_geom_angle_site_symmetry_1
_geom_angle_site_symmetry_3
_geom_angle_publ_flag
C13 P1 C7 114.84(12) . . ?
C13 P1 C1 113.68(12) . . ?
C7 P1 C1 112.37(12) . . ?
C21 O7 C20 114.0(3) . . ?
C2 C1 C6 118.7(2) . . ?
C2 C1 P1 117.87(19) . . ?
C6 C1 P1 123.39(19) . . ?
O1 C2 C3 122.5(2) . . ?
O1 C2 C1 117.3(2) . . ?
C3 C2 C1 120.2(2) . . ?
C2 C3 C4 119.5(3) . . ?
C5 C4 C3 121.8(3) . . ?
C4 C5 C6 119.3(3) . . ?
O2 C6 C5 122.7(2) . . ?
O2 C6 C1 116.7(2) . . ?
C5 C6 C1 120.6(2) . . ?
C8 C7 C12 118.2(2) . . ?
C8 C7 P1 118.4(2) . . ?
C12 C7 P1 123.2(2) . . ?
O3 C8 C9 123.2(3) . . ?
O3 C8 C7 116.2(2) . . ?
C9 C8 C7 120.6(3) . . ?
C10 C9 C8 119.6(3) . . ?
C9 C10 C11 122.0(3) . . ?
C12 C11 C10 118.5(3) . . ?
O4 C12 C11 118.2(3) . . ?
O4 C12 C7 120.7(2) . . ?
C11 C12 C7 121.1(3) . . ?
C14 C13 C18 118.5(2) . . ?
C14 C13 P1 123.9(2) . . ?
C18 C13 P1 117.6(2) . . ?
O5 C14 C15 122.2(2) . . ?
O5 C14 C13 117.1(2) . . ?
C15 C14 C13 120.7(3) . . ?
C16 C15 C14 119.1(3) . . ?
C15 C16 C17 121.9(3) . . ?
C18 C17 C16 119.3(3) . . ?
O6 C18 C17 123.6(3) . . ?
O6 C18 C13 115.8(3) . . ?
C17 C18 C13 120.5(3) . . ?
O7 C20 C19 113.1(4) . . ?
C22 C21 O7 142.4(8) . . ?

_diffrn_measured_fraction_theta_max   0.995
_diffrn_reflns_theta_full   28.35
_diffrn_measured_fraction_theta_full   0.995
_refine_diff_density_max   0.465
_refine_diff_density_min   -0.400
_refine_diff_density_rms   0.057